



**HAL**  
open science

## Amber- and plant-bearing deposits from the Cenomanian of Neau (Mayenne, France)

Didier Néraudeau, Jean-Paul Saint Martin, Simona Saint-Martin, Laurent  
Jeanneau, Jean-David Moreau, Philippe Marc, France Polette, Damien  
Gendry, John Brunet, Jérôme Tréguier

► **To cite this version:**

Didier Néraudeau, Jean-Paul Saint Martin, Simona Saint-Martin, Laurent Jeanneau, Jean-David Moreau, et al.. Amber- and plant-bearing deposits from the Cenomanian of Neau (Mayenne, France). Bulletin de la Société Géologique de France, 2020, L'ambre, 191, pp.39. 10.1051/bsgf/2020039 . insu-03079117

**HAL Id: insu-03079117**

**<https://insu.hal.science/insu-03079117>**

Submitted on 17 Dec 2020

**HAL** is a multi-disciplinary open access archive for the deposit and dissemination of scientific research documents, whether they are published or not. The documents may come from teaching and research institutions in France or abroad, or from public or private research centers.

L'archive ouverte pluridisciplinaire **HAL**, est destinée au dépôt et à la diffusion de documents scientifiques de niveau recherche, publiés ou non, émanant des établissements d'enseignement et de recherche français ou étrangers, des laboratoires publics ou privés.



Distributed under a Creative Commons Attribution 4.0 International License

## Amber- and plant-bearing deposits from the Cenomanian of Neau (Mayenne, France)

Didier Néraudeau<sup>1,\*</sup>, Jean-Paul Saint Martin<sup>2</sup>, Simona Saint Martin<sup>2</sup>, Laurent Jeanneau<sup>1</sup>, Jean-David Moreau<sup>3</sup>, Marc Philippe<sup>4</sup>, France Polette<sup>1,5</sup>, Damien Gendry<sup>1</sup>, John Brunet<sup>6</sup> and Jérôme Tréguier<sup>7</sup>

<sup>1</sup> Université de Rennes, UMR 6118, Géosciences Rennes, Campus de Beaulieu, avenue du Général Leclerc, 35042 Rennes, France

<sup>2</sup> Centre de Recherche en Paléontologie – Paris, UMR 7207, Muséum national d'Histoire naturelle, Sorbonne Université, CNRS, 8, rue Buffon, 75005 Paris, France

<sup>3</sup> Université de Bourgogne Franche-Comté, UMR 6282, Biogéosciences, 6, boulevard Gabriel, 21000 Dijon, France

<sup>4</sup> Université de Lyon I and LEHNA, UMR 5023, 69622 Villeurbanne, France

<sup>5</sup> Department of Geology, University of Namur, ILEE, Institute of Life, Earth and Environment, 61, rue de Bruxelles, 5000 Namur, Belgium

<sup>6</sup> 5, rue de Bellevue, 35220 Marpiré, France

<sup>7</sup> Musée des Sciences, 21, rue du Douanier Rousseau, 53000 Laval, France

Received: 20 May 2020 / Accepted: 28 September 2020

**Abstract** – A new Cenomanian amber- and plant-bearing deposit has been discovered at Neau, in the Mayenne department (France). The Cenomanian fossiliferous lignites are located in karst filling in a substratum of Cambrian limestones. The amber corresponds mainly to tiny millimetric grains, devoid of arthropod inclusions, but rich in microorganisms, especially the sheathed bacteria *Leptotrichites resinatus*, and containing pollen grains (*Classopollis*) and wood fibers (Araucariaceae or Cheirolepidiaceae). The lignites provide abundant conifer and ginkgoale cuticle fragments (*Frenelopsis*, *Eretmophyllum*) and a lot of palynomorphs (e.g. *Gleicheniidites senonicus*, *Cyathidites*, *Deltoidospora*, *Appendicisporites* and *Cicatricosisporites*). The chemical signature of the amber suggests it was produced by conifers of the extinct family Cheirolepidiaceae. According to the palynological assemblage, the age of the lignites is upper lower Cenomanian or lower mid Cenomanian. The deposit environment corresponded to the upstream portion of a mangrove or the most inner part of a lagoon.

**Keywords:** Palynology / Gymnosperm cuticles / Cheirolepidiaceae / Sheathed bacteria / Amber / Cenomanian / France

**Résumé** – Le site à ambre et plantes du Cénomaniens de Neau (Mayenne, France). Un nouveau site à ambre et plantes du Cénomaniens a été découvert à Neau, en Mayenne (France). Les lignites fossilifères cénomaniens sont localisés dans des remplissages de karsts développés dans des calcaires du Cambrien. L'ambre se présente essentiellement sous forme de grains millimétriques, dépourvus d'inclusions d'arthropode, mais riches en microorganismes, notamment en bactéries gainées de type *Leptotrichites resinatus*, et contenant des grains de pollen (*Classopollis*) et des fibres de bois (Araucariaceae ou Cheirolepidiaceae). Les lignites fournissent d'abondants fragments de cuticules de conifères et de ginkgoales (*Frenelopsis*, *Eretmophyllum*) et une grande quantité de palynomorphes (e.g. *Gleicheniidites senonicus*, *Cyathidites*, *Deltoidospora*, *Appendicisporites* et *Cicatricosisporites*). La signature chimique de l'ambre suggère qu'il a été produit par des conifères de la famille éteinte des Cheirolépidiacées. D'après l'assemblage palynologique, l'âge des lignites est Cénomaniens inférieur tardif ou Cénomaniens moyen basal. L'environnement de dépôt correspondait à la partie amont d'une mangrove ou la partie la plus interne d'un lagon.

**Mots clés :** Palynologie / Cuticules de gymnospermes / Cheirolepidiaceae / Bactéries gainées / Ambre / Cénomaniens / France

\*Corresponding author: [didier.neraudeau@univ-rennes1.fr](mailto:didier.neraudeau@univ-rennes1.fr)

## 1 Introduction

Late Cretaceous amber deposits are well distributed in western France, from the Anjou and Sarthe regions, at the North, (Ecommoy locality in Girard *et al.*, 2013a, 2013b; Hucheloup locality in Fleury *et al.*, 2017) to the Aude department, at the South (Fourtou locality in Girard *et al.*, 2013a, 2013b; see Moreau *et al.*, 2017, for a synthetic map of mid-Cretaceous french amber deposits). The more numerous amber deposits and the more rich in amber are located in the Charentes region, where Cenomanian sands and clays with lignite have been studied in several quarries, road works and coastal outcrops (Néraudeau *et al.*, 2002, 2003, 2005, 2008). Conversely, amber from Mayenne has been the less studied. The only previous works were made by Durand and Louail (1971) about the discovery of a karst filling of fossiliferous Cenomanian lignites and sands in a substratum of Cambrian limestones at Neau, and by Azema *et al.* (1972) who performed a palynological analysis of the sediment. The latter study described lower to mid Cenomanian assemblages dominated by gymnosperm pollen grains and fern spores, and marked by the progressive increase of angiospermous forms. Finally, the rare mentions of Cenomanian amber at Neau have been provided by Durand and Louail (1971), and the few available data were then cited by other authors, such as Girard *et al.* (2013a, 2013b). We present here the first synthesis dedicated to the Cenomanian amber from Neau and its associated botanical macro-, meso- and microremains, along with palaeoenvironmental and stratigraphic considerations.

## 2 Material and methods

### 2.1 Field observations

The Neau quarry is located at about 30 km NW from Laval in the department of Mayenne, NW France (Fig. 1). The quarry is exploited by the *Society Chaux & Dolomie Françaises/Lhoist France Ouest* for the extraction of Cambrian dolomitic limestones and the production of lime.

At the top of the Cambrian limestones, several dissolution cavities are filled by Cenomanian erosive deposits (Figs. 2 and 3). According to the field observations made by the authors, the base of the karsts corresponds generally to a few metres of lignitic sand and clay (CnL facies on Figs. 2A and 3) including large pieces of fossil wood (trunk and branches fragments). The top of the karst filling consists of one to two metres of white sand (CnS facies on Figs. 2A and 3A–B), more or less oxidized and coloured in yellow at the contact with the lignite. Both Cambrian limestone palaeoreliefs and karsts are covered by discordant glauconitic sands (CnG facies on Figs. 2A and 3A–B) including more or less kaolinitic lenses. The base of lignitic deposits contains pyritised foraminifers that testify the coastal marine origin of these sediments (Durand and Louail, 1971). The marine remains disappear at the top of the Cenomanian sandy deposits. The presence of kaolinite indicates a typical lateritic weathering anterior to the Cenomanian (Durand and Louail, 1971). One sample of lignitic clay has been collected at the top of the facies CnL in the main karst (Fig. 3A–B), for palynological analyses. In addition, seven samples recovered from Neau amber-rich lignitic clay in 1972, and 39 corresponding palynological

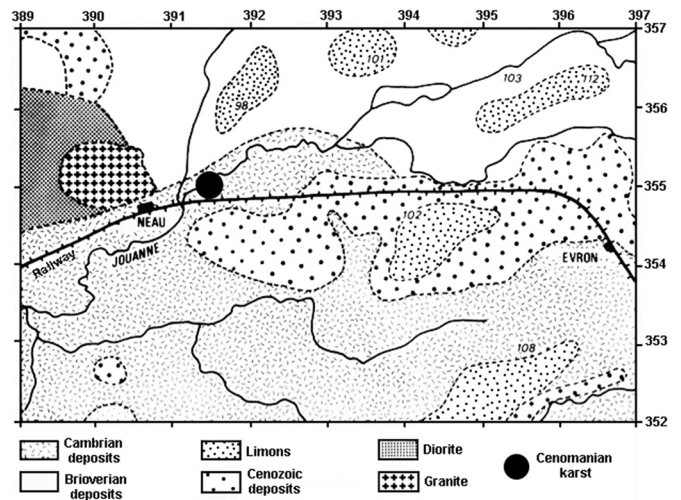


Fig. 1. Simplified geological map of the Neau area, in the Mayenne department, with location of the studied quarry.

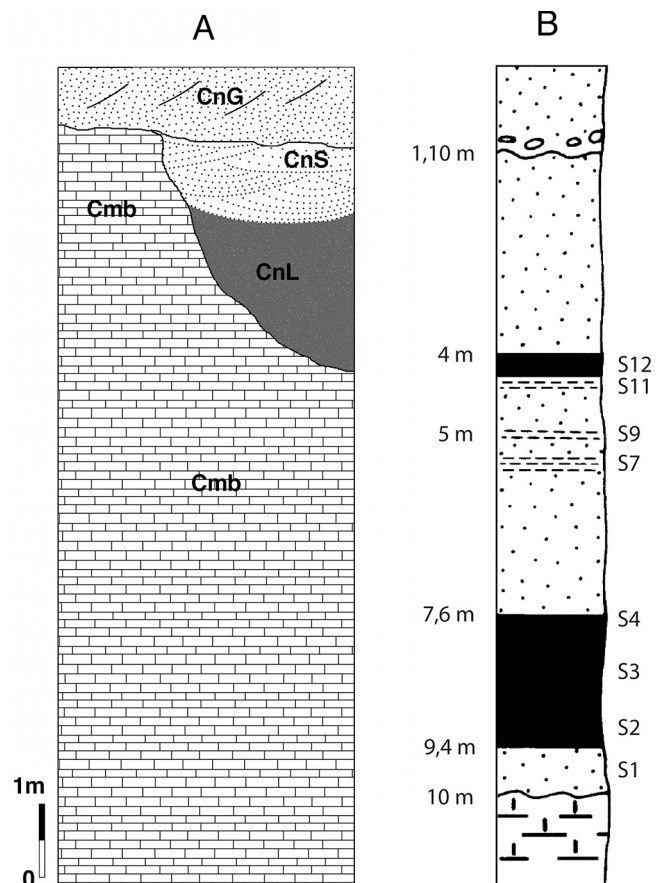


Fig. 2. Geological sections of the Cenomanian karsts from the Neau quarry. A. Synthetic section of the karsts with lignite and amber, observed by the authors (Cmb=Cambrian limestones; CnL=Cenomanian lignites; CnS=Cenomanian sand; CnG=Cenomanian Glauconitic facies). B. Geological section published by Azema *et al.* (1972), with location of their palynological samples S1 to S12.

slides prepared and analyzed by [Azema \*et al.\* \(1972\)](#) were re-examined to complete our palynological analyses and to compare our biostratigraphical and palaeobotanical conclusions (samples S2, S3, S4, S7, S9, S11, S12 on [Fig. 2B](#)).

The amber can be collected by sieving of the lignites, but can also be sometimes collected on the outcrop surface after washout by the rain. The lignites and amber studied in this paper were collected during a field trip organized on June 4th 2014 by the Museum of Laval (J. Tréguier) and the University of Rennes I (D. Néraudeau), completed by additional collections made by John Brunet and D. Gendry.

## 2.2 Amber, wood and cuticle preparation ([Fig. 4](#))

Tiny amber grains have been collected by sieving of the lignitic clay, and then separated from wood and cuticle fragments ([Fig. 4A](#)). The lignitic marl was soaked in a solution of hydrogen peroxide (12%) and water for a few days. The disaggregated sediment was then washed with tap water through a column of sieves (2.0 mm, 1.0 mm and 0.5 mm meshes). The pieces of ambers as well as fossil plants ([Fig. 4B–H](#)) were picked out by naked eye or under a stereomicroscope Leica 125. Photographs were taken with a BMS digital USB camera (5 megapixels). Specimens are housed in the collections of the University of Rennes 1 under numbers IGR-PAL-2828 and IGR-PAL-22829 for the wood fragments and IGR-PAL-2830 to IGR-PAL-2836 and IGR-PAL-2844/IGR-PAL-2845 for the plant cuticles. An amber lot is housed under number IGR-PAL-2843. Amber slides used to illustrate the amber inclusions correspond to numbers IGR-PAL-2837 to IGR-PAL-2842. The amber grain containing wood fragments studied in the paper corresponds to number IGR-PAL-2846.

In the lignitic clay, plant remains are greatly disarticulated and vary in size including meso- to macro-remains ([Fig. 4B–H](#)). They consist of leafy axes ([Fig. 4B–E](#)) and cone scales of conifers ([Fig. 4F](#)) as well as fragmented leaves of ginkgo-phytes ([Fig. 4G, H](#)). Wood fragments are also abundant ([Fig. 4A](#)). The collection includes hundreds of plant specimens. They are preserved as coalified compressions with or without cuticles. Some plant microremains (pollen, woods) were also found as inclusions inside amber.

In order to characterize the amber grains, thin sections were prepared with a thickness slightly greater than the standard thickness of the petrographic thin section. The optical microscope used is a Zeiss Axioscope 40 with photographing device and observations were made with  $\times 5$  and  $\times 10$  objectives for large observation. The observations under confocal laser scanning microscope (CLSM) were essentially performed on a Leica TCS SP5 microscope. The images obtained allow viewing of the autofluorescent objects in false colours. 3D reconstruction was obtained by acquisition of stacks of closely spaced confocal optical sections at 0.10  $\mu\text{m}$  to 0.20  $\mu\text{m}$  intervals. Then these images were treated for optimization with the open source software Image J ([Rasband, 1997–2013](#)). Amber and wood examinations with Scanning Electron Microscope (SEM) were performed with the Hitachi SU3500 model.

In addition to the micro-fragments of wood found by sieving of the lignitic clay ([Fig. 4A](#)), several large pieces of



**Fig. 3.** Lignite and amber deposits from the Neau quarry. A. General view showing the Cenomanian lignites (CnL) in karsts incising the Cambrian limestones (Cmb); at the top of the quarry, Cenomanian glauconitic sands overlap both Cenomanian white sands (CnS) and Cambrian limestones. B. One Cenomanian karst showing at its top the contact between the lignites containing amber (CnL) and the glauconitic sands (CnG); the bag of the collector contains a large piece of fossil wood. C. Lateral view of a Cenomanian karst with the lignites (CnL) directly in erosive contact with the Cambrian limestones (Cmb) (photographs D. Néraudeau).

trunk and branches have been collected during the field trip at the surface of the outcrop ([Fig. 3B](#)).

## 2.3 Amber analyses

Two pieces of Neau amber, an opaque and milky denoted form A and a translucent and orange denoted form B and a yellowish Baltic amber as reference were analyzed by thermally assisted hydrolysis and methylation (THM) also called thermochemolysis. Small portions of amber were crushed manually in an agate mortar. The powders ( $\sim 0.1$  mg) were heated with TMAH (Tetramethylammonium Hydroxyde) at 400°C. THM was carried out using a Frontier Lab PY-2020iD pyrolyser coupled with a Shimadzu GCMS-QP2010 Plus system operating with a split ratio of 100. Separation was achieved using a capillary column SLB-5MS (60 m  $\times$  0.25 mm ID, 0.25  $\mu\text{m}$  film thickness) with the carrier gas He with a flow of 1.1 mL/min. The operating conditions were as follows:

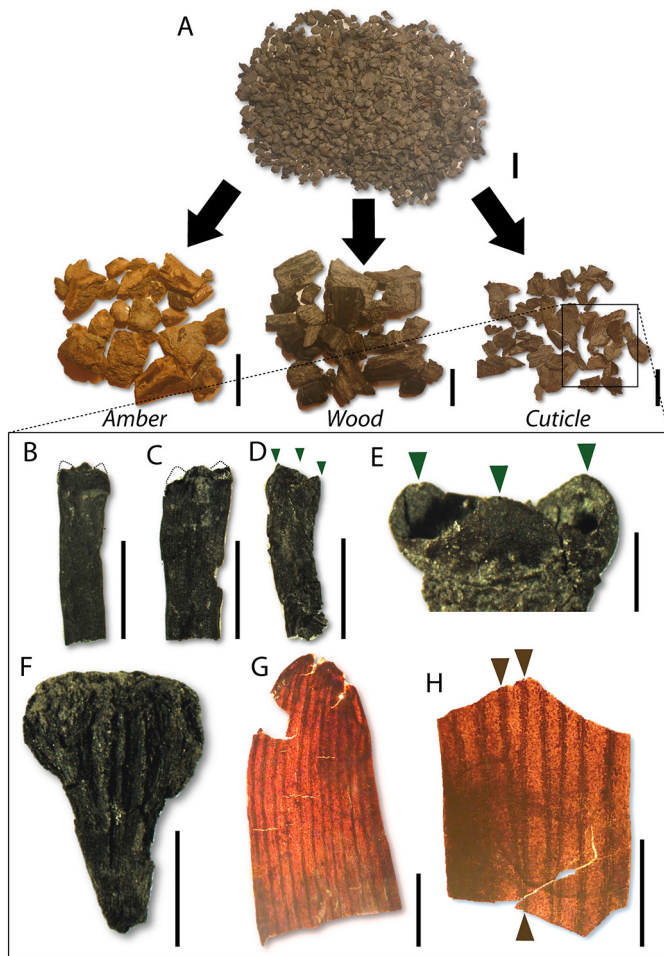


**Fig. 4.** A. Amber, cuticle and wood remains extracted after soaking of sediment in a solution of hydrogen peroxide. B–E. Leafy axes of the conifer *Frenelopsis* sp. showing the characteristic tree short parts of the leaves (located by arrows), IGR-PAL-2830 to IGR-PAL-2833. F. Conifer cone scale IGR-PAL-2834. G–H. Fragments of leaves ascribed to *Eretmophyllum obtusum* showing the characteristic bifid veins (located by arrows), IGR-PAL-2835 and IGR-PAL-2836. Scale bars: A = 1 cm; B–D and G–H = 5 mm; E = 1 mm; F = 2 mm.

initial temperature held at 50 °C for 2 minutes, increased to 310 °C at a rate of 4 °C/min for 34 minutes. Individual compounds were identified based on comparison of (i) MS data with the NIST2014 library and literature (Anderson, 1994, 1996, 2006; Dutta *et al.*, 2011; Otto and Simoneit, 2002) and (ii) retention time with the reference Baltic amber.

The relative distribution of identified compounds was determined by measuring the area of a specific fragment, denoted  $m/z$  integration in Table 1. The peak area of the selected  $m/z$  for each compound was integrated and corrected by a mass spectra factor (Tab. 1) calculated as the reciprocal of the proportion of the fragment used for the integration and the entire fragmentogram. The molecular ratios were calculated using those corrected areas that allow an approximation of areas on the total ion chromatogram while preventing from the integration of co-eluting compounds.

## 2.4 Palynomorphs

Seven samples were recovered from Neau amber-rich lignitic clay in 1972, and 39 corresponding palynological slides were prepared and analyzed by Azema *et al.* (1972; S2, S3, S4, S7, S9, S11, S12, see Fig. 2B). Because their study focused on several Cenomanian localities of western France, Azema *et al.* (1972) chose not to discuss extensively the palaeoenvironmental implications and the age attribution of the palynological assemblages of Neau. The palynomorphs illustrated are not accompanied by coordinates, and one cannot know which pollen grain or spore comes from Neau or from another locality. Thus, in order to determine more precisely the palaeoenvironmental and stratigraphic modalities associated with the formation/deposit of Neau resin – and later amber –, those 39 slides were re-examined, and the corresponding results are presented herein.

Several slides now correspond to partly dried residue, rendering observations difficult, but all seven samples yielded palynological assemblages, however often small. If the sample and corresponding slides were not particularly rich, all palynomorphs were counted and identified, as it is the case for S2 (N = 132), S7 (N = 27), S9 (N = 23), S11 (N = 135), and S12 (N = 106). The two remaining samples S3 and S4 provided rich assemblages. Three hundred palynomorphs were counted and identified, but all the palynomorphs were observed in order to log potential infrequent forms (Appendix S1). The 39 slides are housed in the collections of the University of Rennes 1 under numbers Cd1 to Cd39.

## 3 Plant remains from the lignitic clay

### 3.1 Coalified compressions and cuticles from the lignitic clay

#### Conifers

Family Cheirolepidiaceae

Genus *Frenelopsis* Schenk, 1869 emend. J. Watson, 1976

*Frenelopsis* sp.

(Fig. 4B–E)

**Material.** Forty-three specimens, from which IGR-PAL-2830 to IGR-PAL-2833 are figured.

**Description.** The material consists of isolated internodes constituting the leafy axes (Fig. 4B–D). The internodes are never connected. They are elongated, flattened, up to 13.0 mm long, and up to 3.5 mm wide. Each internode is formed by one whorl of three proximally fused leaves. Free parts of the leaves are only visible distally (Fig. 4B–E). They form three tiny tips which are triangular in shape, broader than long, up to 1.0 mm long, and up to 2.5 mm wide and show an obtuse apex (Fig. 4E). Surface of internodes shows numerous longitudinal rows of stomata.

**Remarks.** Cellular characters of the stomata are not preserved. *Frenelopsis* is one of the most abundant conifers from the Cenomanian deposits of Western France. This taxon was reported from many areas in Aude, Charente-Maritime, Vienne and Maine-et-Loire (see synthesis in Moreau *et al.*, 2017 and references therein).

#### Family Incertae sedis

Cone scale Type 1

(Fig. 4F)

**Table 1.** List of identified compounds and their relative proportions in Neau ambers. Target compounds were identified based on m/z int and m/z identification. Areas were integrated using the m/z int, and the area on the total ion chromatogram was estimated using the mass spectra factor (MSF). Non-detected compounds are denoted “*n.d.*”.

No.	Compound name	m/z identification	m/z int	MSF	Form A	Form B
1	Naphthalene-1,2,3,4,4a,7,8,8a-octahydro-1,4a,6-trimethyl (IVe)	81, 107, 163, 178	163	9	1.8	1.3
2	Naphthalene-1,2,3,4,4a,7,8,8a-octahydro-1,4a,6-trimethyl (IVf)	95, 163, 178	163	17	2.4	2.4
3	Naphthalene-1,2,3,4,4a,5,8,8a-octahydro-1,4a,6-trimethyl (Ve)	81, 107, 163, 178	163	14	0.6	0.6
4	Dimethyltetralin	145, 160	145	4	0.7	1.3
5	Naphthalene-1,2,3,4,4a,5,8,8a-octahydro-1,4a,6-trimethyl (Vf)	95, 163, 178	163	13	0.3	0.3
6	Trimethyltetralin	159, 174	159	4	0.2	0.3
7	Naphthalene-1,2,3,4,4a,7,8,8a-octahydro-1,1,4a,6-tetramethyl (IVc)	81, 95, 107, 177, 192	177	12	0.6	0.4
8	Naphthalene-1,2,3,4,4a,5,8,8a-octahydro-1,1,4a,6-tetramethyl (Vc)	95, 121, 177, 192	177	11	0.2	0.2
9	Trimethylindene	143, 158	158	8	0.5	1.7
10	Naphthalene-1,2,3,4,4a,7,8,8a-octahydro-1,4a,5,6-tetramethyl (VIe)	95, 121, 177, 192	177	9	2.5	2.0
11	Dimethylnaphthalene isomer	141, 156		6	1.1	3.1
12	Naphthalene-1,2,3,4,4a,5,8,8a-octahydro-5-methylene-1,4a,6-trimethyl (VIIe)	108, 175, 190	175	12	4.6	3.2
13	Dimethylnaphthalene isomer	141, 156	141	6	0.3	0.9
14	Naphthalene-1,2,3,4,4a,7,8,8a-octahydro-1,4a,5,6-tetramethyl (VI f)	95, 121, 177, 192	177	11	0.9	1.0
15	Naphthalene-1,2,3,4,4a,5,8,8a-octahydro-5-methylene-1,4a,6-trimethyl (VII f)	93, 175, 190	175	13	1.5	1.5
16	Ionene	159, 174	159	4	<i>n.d.</i>	3.6
17	Naphthalene-1,2,3,4,4a,7,8,8a-octahydro-1,1,4a,5,6-pentamethyl (VIc)	95, 121, 191, 206	191	16	1.1	0.9
18	Methylionene	173, 188	173	4	0.6	2.1
19	Naphthalene-1,2,3,4,4a,5,8,8a-octahydro-1,1,4a,6-tetramethyl-5-methylene (VIIc)	105, 119, 161, 204	204	15	<i>n.d.</i>	0.8
20	Timethyldihydronaphthalene isomer	142, 157, 172	157	4.6	<i>n.d.</i>	0.3
21	Naphthalene-1,2,3,4,4a,7,8,8a-octahydro-1-methoxymethyl-1,4a,6-trimethyl methyl ester (IVd)	95, 107, 177, 222	177	17	0.4	<i>n.d.</i>
22	Trimethylnaphthalene isomer	155, 170	155	5	0.1	0.3
23	Timethyldihydronaphthalene isomer	142, 157, 172	157	4.6	0.5	2.0
24	Timethyldihydronaphthalene isomer	142, 157, 172	157	4.6	0.2	0.6
25	Trimethylnaphthalene isomer	155, 170	155	5	0.1	0.4
26	Trimethylnaphthalene isomer	155, 170	155	5	0.1	0.5
27	Trimethylnaphthalene isomer	155, 170	155	5	0.1	0.4
28	Naphthalene-1-carboxylic acid-1,2,3,4,4a,7,8,8a-octahydro-1,4a,6-trimethyl methyl ester (IVa)	161, 177, 236	177	19	5.3	<i>n.d.</i>
29	Trimethylnaphthalene	155, 170	155	5	2.6	9.6
30	Naphthalene-1-carboxylic acid-1,2,3,4,4a,5,8,8a-octahydro-1,4a,6-trimethyl methyl ester (Va)	176, 121, 161	161	23	2.4	0.2
31	Naphthalene-1,2,3,4,4a,7,8,8a-octahydro-1-methanol-1,4a,6-trimethyl methyl ester (IVb)	177, 95, 208	177	10	0.2	0.2
32	Tetramethylnaphthalene isomer	169, 184	169	5	0.6	1.9
33	Naphthalene-1,2,3,4,4a,5,8,8a-octahydro-1-methanol-1,4a,6-trimethyl methyl ester (Vb)	55, 109, 177, 208	177	40	0.3	<i>n.d.</i>

**Table 1.** (continued).

No.	Compound name	m/z identification	m/z int	MSF	Form A	Form B
34	Naphthalene-1,2,3,4,4a,7,8,8a-octahydro-1-methoxymethyl-1,4a,5,6-tetramethyl methyl ester (VIId)	109, 121, 189, 236	121	18	0.5	<i>n.d.</i>
35	Tetramethylnaphthalene isomer	169, 184	169	5	0.1	0.5
36	Naphthalene-1,2,3,4,4a,5,8,8a-octahydro-1-methoxymethyl-1,4a,6-trimethyl-5-methylene (VIIId)	132, 187, 234	132	15	1.3	<i>n.d.</i>
37	Tetramethylnaphthalene isomer	169, 184	169	5	0.1	0.4
38	Tetramethylnaphthalene isomer	169, 184	169	5	0.3	0.9
39	Naphthalene-1-carboxylic acid-1,2,3,4,4a,7,8,8a-octahydro-1,4a,5,6-tetramethyl methyl ester (VIa)	175, 191, 235, 250	175	11	13.9	1.1
40	Naphthalene-1-carboxylic acid-1,2,3,4,4a,5,8,8a-octahydro-1,4a,6-trimethyl-5-methylene methyl ester (VIIa)	173, 133, 188, 248	173	9	20.4	0.9
41	Amberene	159, 215, 230	159	3.5	<i>n.d.</i>	0.2
42	Naphthalene-1,2,3,4,4a,7,8,8a-octahydro-1-methanol-1,4a,5,6-tetramethyl methyl ester (VIb)	95, 191, 207, 222	191	27	0.9	1.3
43	Naphthalene-1,2,3,4,4a,5,8,8a-octahydro-1-methanol-1,4a,6-trimethyl-5-methylene (VIIb)	91, 132, 187, 220	132	20	1.5	1.4
44	16,17,19-Trisnorabieta-8,11,13-triene	131, 157, 213	131	7	3.5	4.8
45	16,17,18-Trisnorabieta-8,11,13-triene	131, 157, 213	131	7	1.9	3.2
46	Bisnorsimonellite isomer	179, 209, 224	209	4.9	0.6	1.9
47	16,17-Bisnordehydroabietane	131, 145, 157, 227, 242	227	16	1.1	1.3
48	7-Oxo-16,17,18-trisnorabieta-8,11,13-triene	145, 227, 242	145	6	0.3	0.4
49	Bisnorsimonellite isomer	179, 209, 224	209	4.9	0.3	0.8
50	19-Norabietatriene	159, 241, 256	159	7	<i>n.d.</i>	0.8
51	18-Norabietatriene	159, 241, 256	159	7	0.3	0.8
52	Dimethylphenanthrene	206, 191	206	6	5.3	15.1
53	Trimethylphenanthrene isomer	220, 205	220	7	0.2	0.7
54	Trimethylphenanthrene isomer	220, 205	220	7	0.4	1.8
55	Trimethylphenanthrene isomer	220, 205	220	7	0.5	1.4
56	Trimethylphenanthrene isomer	220, 205	220	7	0.2	1.3
57	Trimethylphenanthrene isomer	220, 205	220	7	0.1	0.5
58	Methyl 16,17-dinorcallitrisate	211, 271, 286	211	5	2.0	0.5
59	Methyl isopimarate	241, 257, 274, 301, 316	241	9	0.4	<i>n.d.</i>
60	Methyl 17-norcallitrisate	225, 285, 300	225	5	0.1	<i>n.d.</i>
61	Methyl 16,17-dinordehydroabietate	211, 271, 286	211	5	6.3	2.1
62	Methyl pimara-8,15-dien-18-oate	241, 257, 287, 316	241	15	0.4	<i>n.d.</i>
63	Methyl 8-abieten-18-oate	243, 259, 303, 318	243	13	4.2	2.9
64	Methyl 17-nordehydroabietate	225, 285, 300	225	5	0.3	0.1
65	Methyl callitrisate	239, 299, 314	239	4	<i>n.d.</i>	2.3
66	Methyl dehydroabietate	239, 299, 314	239	4	0.1	6.3

*Material.* One specimen, IGR-PAL-2834.

*Description.* The scale is longer than wide (*i.e.*, 4.5 mm long and 3 mm wide), convex, shows an acuminate base, a broad truncate apex and an entire margin (Fig. 4F). The base displays a long free stalk (2.5 mm long and up to 1.5 mm wide). The adaxial surface displays several central and proximal grooves. They end before the truncate apex.

*Remarks.* The preservation is not sufficient to unambiguously identify the presence of ovule scars. Some isolated

ovulate cone scales were previously reported from the lower Cenomanian of western France, in Charente-Maritime (*e.g.*, Néraudeau *et al.*, 2009). They were tentatively ascribed to *Alvinia bohémica* (Velen.) J. Kvaček. However, the shape of the cone scale from Mayenne differs from these specimens.

#### Ginkgoales

Family Karkeniaceae

Genus *Eretmophyllum*

*Eretmophyllum obtusum* (Velen.) J. Kvaček, (1999)

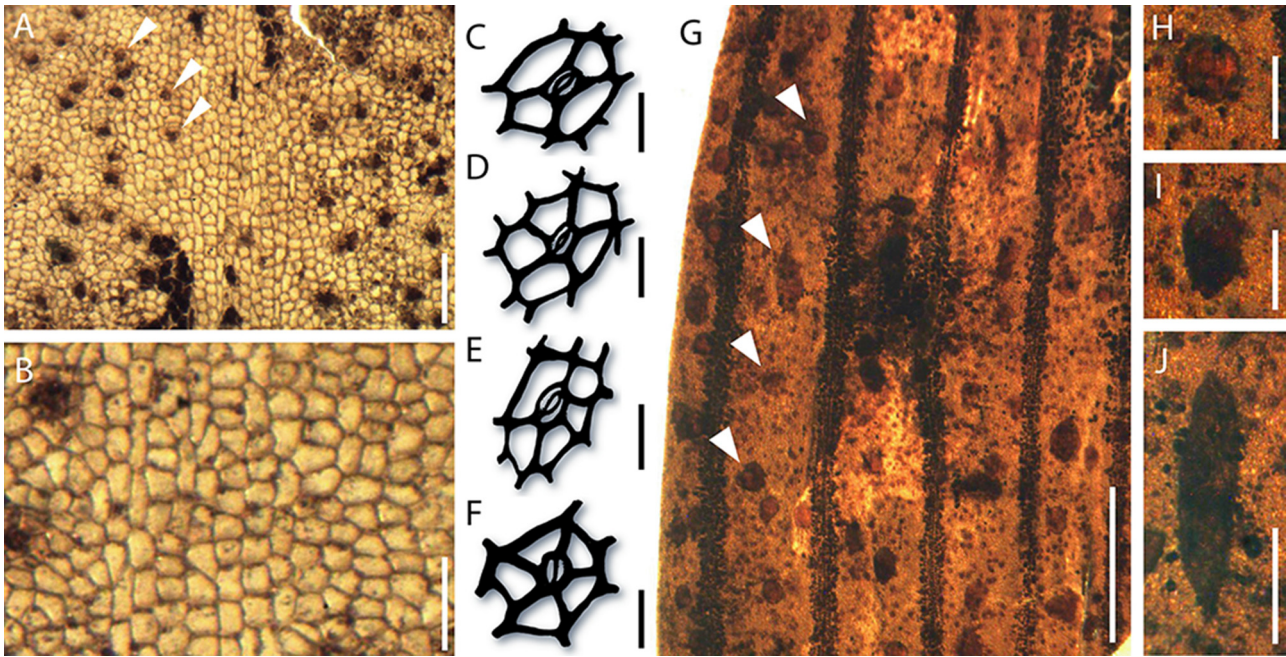


**Fig. 5.** *Eretmophyllum obtusum*. A–B. Details of cuticle showing the arrangement of cells, and the random orientation of stomatal apparatuses (white arrows), IGR-PAL-2844. C–F. Sketches of stomatal apparatuses showing arrangement of subsidiary cells. G. Arrangement of resin bodies (white arrows) preserved in the mesophyll between veins IGR-PAL-2845. H–J. Rounded and spindle-shaped resin bodies. Scale bars: A and H–J = 500  $\mu\text{m}$ ; B = 200  $\mu\text{m}$ ; C–F = 100  $\mu\text{m}$ ; G = 2 mm.

(Fig. 4G–H and Fig. 5A–J)

**Material.** Sixteen specimens, from which IGR-PAL-2835 and IGR-PAL-2836 are figured.

**Description.** The material consists of up to 20 mm long and up to 11 mm wide fragmented lamina (Fig. 4G–H). The leaves are coriaceous and entire-margined. The apices are obtuse. Base of leaves and petiole are not preserved. The veins are dichotomously branched and run subparallel to leaf lamina and converge near the apex (Fig. 4G–H). The dichotomies form narrow angles. In the medial part, lamina display up to 12 parallel veins. The veins are up to 0.3 mm wide and are regularly spaced. Cuticle is heavily cutinized. Cuticle displays costal and intercostal bands, both bearing stomata apparatuses. Leaves are amphistomatic. Stomata are randomly oriented, scattered, and particularly abundant in intercostal bands (Fig. 5A). Stomata are haplocheilic, sunken and surrounded by 4 to 6 subsidiary cells (Fig. 5C–F). The diameter of stomatal apparatuses varies from 40 to 70  $\mu\text{m}$ . The stomatal pits show a round or oval shape. Ordinary epidermal cells are square, rectangular, or polygonal, 20–110  $\mu\text{m}$  long and form longitudinal rows. The anticlinal walls of ordinary epidermal cells are straight to slightly sinuous (Fig. 5B). Numerous rounded and spindle-shaped resin bodies are dispersed in the mesophyll (Fig. 5G). Rounded ones are up to 0.5 mm in diameter whereas spindle-shaped ones are up to 1.1 mm long (Fig. 5H–J).

**Remarks.** Pons *et al.* (1976) erected the species *Eretmophyllum andegavense* D.Pons, Boureau et Broutin based on material from the Cenomanian of Angers (western France). However, the distinction of *Eretmophyllum* (Velen.) J.Kvaček

with *Nehvizdya* Hlušík is debated for a long time. Kvaček (1999) transferred *Nehvizdya* to the genus *Eretmophyllum*, and introduced a new combination, *Eretmophyllum obtusum* (Velen.) J.Kvaček. However, Gomez *et al.* (2000) attempted to distinguish *Eretmophyllum* from *Nehvizdya* on the basis of the presence or absence of papillae on subsidiary cells as the differential character. Gomez *et al.* (2000) tentatively transferred the species *Eretmophyllum andegavense* in the genus *Nehvizdya*. However, as pointed by Kvaček *et al.* (2005) the differential character used by Gomez *et al.* (2000) is not acceptable being variable among genera in the Ginkgoales. Here, we follow Kvaček *et al.* (2005) who suggested that *Nehvizdya* and *Eretmophyllum* cannot be splitted only based on the “papillae” argument. Although several studies (Gomez *et al.*, 2004, 2008; Néraudeau *et al.*, 2005) reported *Nehvizdya andegavense* from the Albian–Cenomanian of several localities in Charente-Maritime, we agree with Fleury *et al.* (2017) who used *Eretmophyllum* rather than *Nehvizdya* for material from the Cenomanian of western France (Maine et Loire).

### 3.2 Palynomorphs from the lignitic clay

The seven palynological samples yielded a fairly diverse palynoflora composed of 71 species and ca. 1000 specimens (Appendix S1). Abundance charts of the five richest samples show that the proportion between spores (Fig. 6C–L) and pollen grains (Fig. 6M–Z) is well balanced, but spores are often slightly dominant (Fig. 6A). They usually represent around 60% of the assemblage, but can go up to 92% for S4. Most abundant spores correspond to *Gleicheniidites senonicus*

(Gleicheniaceae), to smooth walled forms associated with the genera *Cyathidites* and *Deltoidospora*, and to massive cicatricose spores of *Appendicisporites* and *Cicatricosisporites* (Anemiaceae; Fig. 6A, E–J). *Appendicisporites insignis* (Fig. 6I–J) is the most common form of ornamented spores. Among subsidiary spores are those of the Lycophytes, mostly belonging to *Camarozonosporites* (Fig. 6D), a few bryophytic forms (Fig. 6C), spores associated with the Osmundaceae, such as *Baculatisporites* (Fig. 6K), and spores of uncertain botanical affinities, like *Patellaspores tavadensis* (Fig. 6L) and *Microreticulatisporites sacalii*.

Gymnosperm pollen grains (Fig. 6M–O) are dominated by Circumpolles (*Classopollis torosus*) and small inaperturate or monoaperturate grains associated with the Cupressaceae (incl. Taxodiaceae), including *Exesipollenites tumulus*, *Inaperturopollenites dubius*, and *Taxodiaceapollenites hiatus* (Fig. 6A). On the contrary, bisaccates (mostly Pinaceae/Podocarpaceae, Fig. 6M) and grains of Araucariaceae (*Araucariacites*, Fig. 6N) were rarely encountered, and seldom represent more than 5% of the assemblages, except for the youngest assemblage (Fig. 6A).

While the different groups of spores and gymnosperm pollen grains display a fairly fluctuant abundance throughout the five assemblages, S11 and S12 are marked by the sudden increase of angiosperm pollen grains (Fig. 6A). They represent from 3–5% of S2–S4 to 12–15% of S11–S12. Numerous representatives of *Dichastopollenites* were observed (uncertain affinity), as well as tricolpate (*Tricolpites*, Fig. 6V), tricolporate (*Nyssapollenites*, Fig. 6U), and tricolpoidate (*Phimopollenites*, Fig. 6X–Z) forms belonging to the Eudicots. Grains of *Phimopollenites* were particularly diversified and abundant. Less common forms include *Stellatopollis* cf. *largissimus* (Fig. 6S) and *Artiopollis indivisus* (Fig. 6T). No normapollens were observed. Very few dinocysts were logged in the oldest assemblages, mostly belonging to *Surculosphaeridium longifurcatum* (Fig. 6B). Except for the progressive increase of the abundance of the angiosperm pollen grains, and the curious abundance peak of *Glecheiniidites* in S4, no particular trend is noticed from S2 to S12, and the resulting interpretation will therefore consider the “Neau palynoflora” as a whole.

## 4 Amber characteristics

### 4.1 General aspect (Figs. 7 and 8)

The collected amber grains are of variable appearance and size. Large pieces of amber are very uncommon and have been collected at the surface of the outcrop. They range from 1 to 3 cm in size. Three varieties of colour have been observed: milky brown (Fig. 7A), translucent honey (Fig. 7B) and opaque cork colour (Fig. 7C–D). A few ones are empty (Fig. 7D). The size of tiny amber grains collected by clay sieving varies generally from a few millimetres to one centimetre (Fig. 8A). Then, the appearance of the grains depends on the shape of the original resin drops or their posterior fragmentation, during transport or the conditions of deposit and sampling. Thus, the best preserved grains correspond to fine, more or less cylindrical flows or rather spherical drops with an attachment point. Others result from a

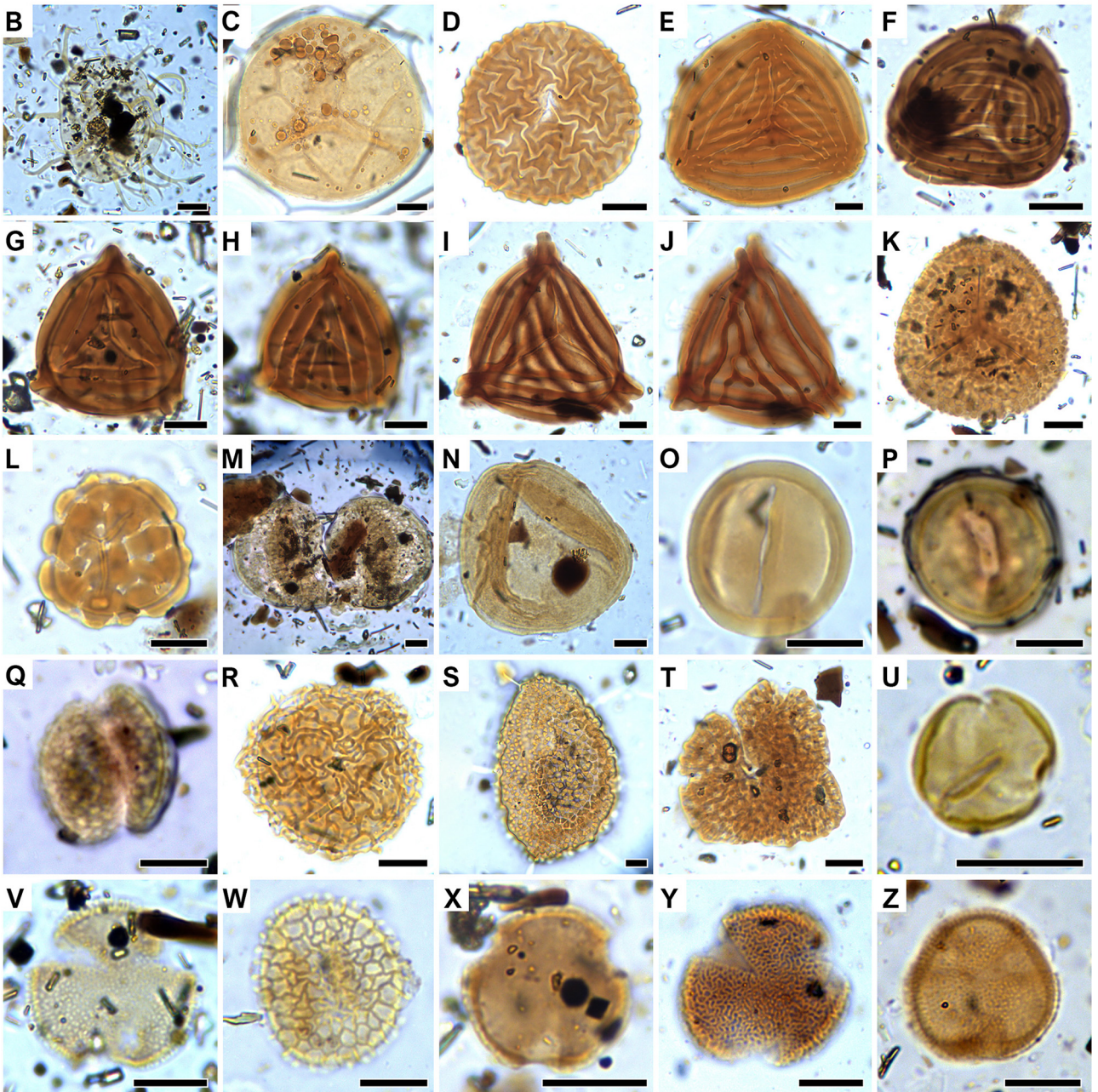
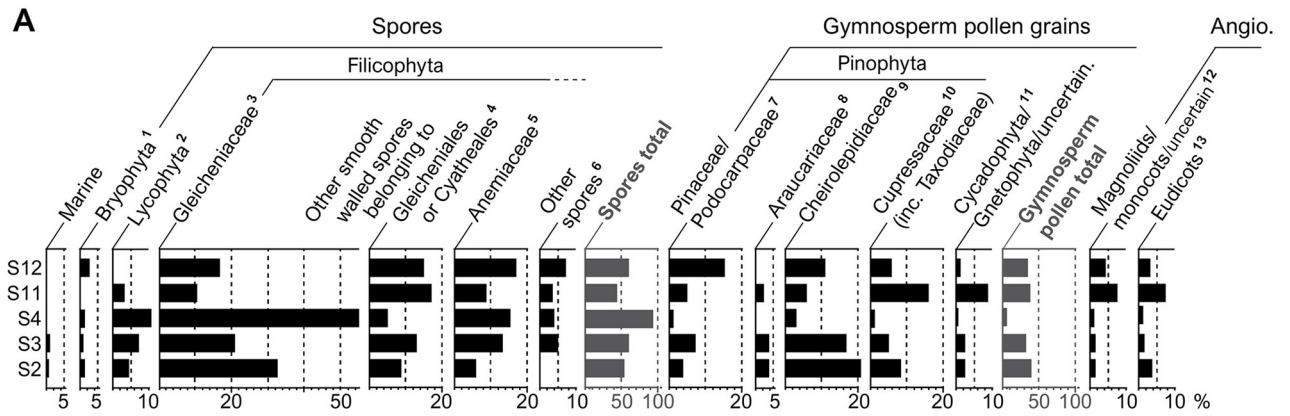
more complex flow and show several protuberances. If some grains appear translucent with a dominant orange-yellow colour, very many grains are wholly or partly opaque with earthy or cork colours of beige to brown (Figs. 4A and 8A). The opacity is very irregularly distributed according to the grains appearance (Fig. 8B–E) corresponding to several phenomena: presence of bubbles and/or emulsions more or less coarse, colonization by filamentous microorganisms (Fig. 8H) or a conjugation of both (Fig. 8B, I). The external appearance revealed by the SEM observations shows that cracks are often present on the surface of the amber grains (Fig. 8F). In some cases the superposition of resin flows is clearly visible (Fig. 8G).

### 4.2 Plant microremains included inside amber

#### 4.2.1 Vegetal fibers and wood (Fig. 9)

The size of the large pieces of wood collected on the outcrop varies from several centimetres to about 1 m, and numerous ones show *Teredo*-borings typical for coastal marine environments in transgressive settings (Gingras *et al.*, 2004), and tiny borings of unknown origin (*Teredo*, insect attacks?) (Fig. 9A, B). SEM observations of the wood fragments included in the amber evidenced pitting on the radial tracheid walls, preserved as pit chamber inner casts (Fig. 9C, D). While some up to 9 pits long row of contiguous pits occurred (Fig. 9D), locally pit rows seems to be interrupted (Fig. 9C). The regularity of the spacing between the preserved pits, however, argues more for non-preservation than for absence of pits. Consequently the tracheid radial pitting was interpreted as araucarian. The cross-fields are of the araucarioid type, with 5 to 7 contiguous alternate cupressoid oculipores (Fig. 9E). The fragmentary material did not allow to study growth-ring features, nor the occurrence or resin canals or axial parenchyma. According to these limited morphological observations, the most probable taxa are (from the most probable to the least one) (1) *Agathoxylon*; (2) *Brachyoxylon*; (3) *Ginkgoxylon*. The fact that these wood pieces are included in the amber could indicate that the resin producers were Araucariaceae or Cheirolepidiaceae. These are indeed the only wood genera yet reported from the Mesozoic and combining araucarioid cross-fields and at least partly araucarian radial tracheid pitting (Philippe and Bamford, 2008).

All these three genera are known to produce resin inside their tracheids (Philippe, 1995), and the three of them were reported from the Cenomanian of Western France (Perrichot, 2005). The first and xylologically most probable one, *Agathoxylon*, was reported associated to all ambers with the same provenance. Despite its etymology genus *Agathoxylon* is not necessarily a univocal evidence of the Araucariaceae. After this has been suspected several times, it has recently been shown that *Agathoxylon* wood can also occur in Cheirolepidiaceae (Stewart *et al.*, submitted). *Brachyoxylon* is usually considered as related to the Cheirolepidiaceae (Macchour and Pons, 1995) and *Ginkgoxylon* to the Ginkgoalean (Jiang *et al.*, 2016). Here in Neau, according to the non-woody remains all the three taxa occur (*i.e.* Araucariaceae, Cheirolepidiaceae and Ginkgoalean). The amber-embedded fragment of wood therefore does not make it possible to specify the taxonomic origin of this amber.



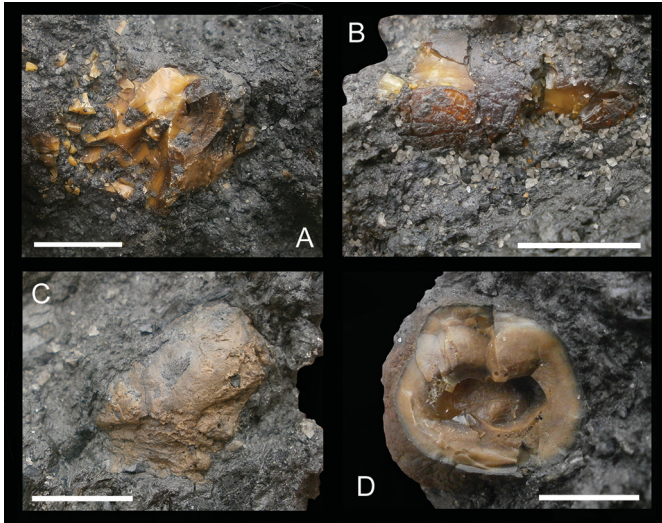


**Fig. 7.** Large amber pieces from the Neau quarry. A. Milky brown variety. B. Translucent honey variety. C. Cork colour variety. D. Empty piece of cork colour variety; note the black colouring of the peripheral part, linked to the proliferation of the sheathed bacteria *Leptotrichites resinatus*. Scale bar = 10 mm.

#### 4.2.2 Pollen grains included in amber (Fig. 10)

Examination of some thin sections revealed the presence of gymnosperm pollen grains belonging to the genus *Classopollis*, which is associated with the extinct family of the Cheirolepidiaceae (Balme, 1995; Schrank, 2010; Fig. 10). They are often arranged in clusters (Fig. 10A–B, F), but isolated grains were also observed (Fig. 10C–D). Their rimula is discrete, but discernable. Azema *et al.* (1972) found numerous *Classopollis* grains within the lignitic clay of Neau, that they all identified as a new species called *Classopollis tenuiparietalis*. However, they state that *C. tenuiparietalis* is morphologically identical to the Aptian and Cenomanian Portuguese taxon *Classopollis obidosensis* Groot and Groot,

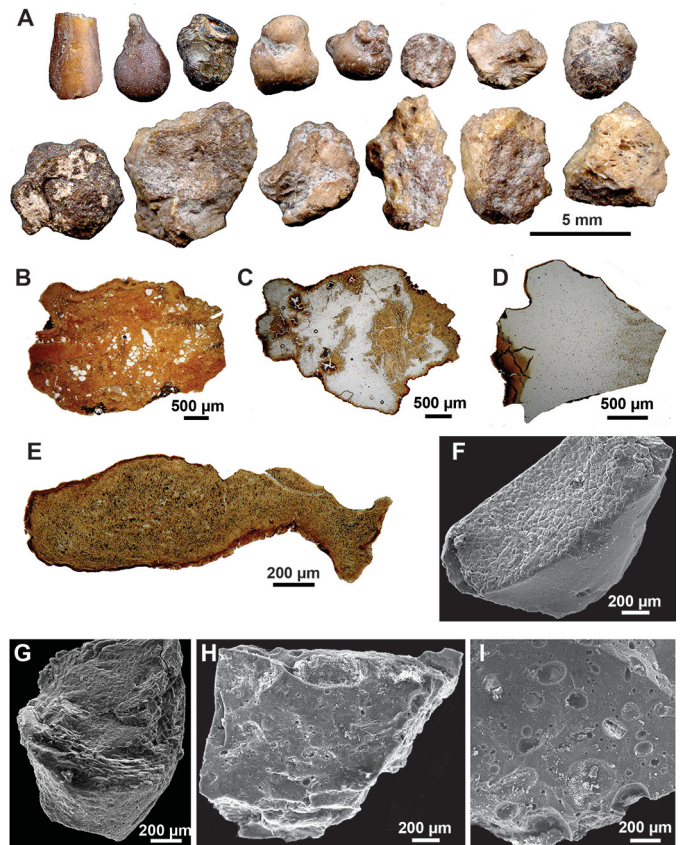


**Fig. 8.** Amber features. A. Forms and aspects of the collected amber grains, some having kept the characteristics of the original resin drops; note the abundance of opaque grains with earthy colours. B–E. Sections of grains in thin sections showing various situations of more or less opaque grains. F. Cracked external surface of a grain under SEM. G. Stack of resin flows within a grain. H. Opaque grains marked by dense filamentous networks. I. Opaque grain containing many bubbles and colonization by filamentous networks.

**Fig. 6.** A. Abundance charts of the most productive palynological assemblages from the amber-rich lignitic clays of Neau. Charts are based on the botanical affinities of the various spores and pollen morphotypes. Encountered genera: 1: *Aequitriradites*, *Stereisporites*, *Triporoletes*; 2: *Camarozonosporites*, *Densoisporites*, *Retitriletes*; 3: *Gleicheniidites*, *Ornamentifera*; 4: *Cyathidites*, *Deltoidospora*, *Dictyophyllidites*, *Matonisporites*, *Toroisporis*; 5: *Appendicisporites*, *Cicatricosisporites*, *Distaltriangulisporites*; 6: *Auritulinasporites*, *Baculatisporites*, *Concavissimisporites*, *Laevigatosporites*, *Microreticulatisporites*, *Patellasporites*, *Todisporites*; 7: *Parvisaccites*, *Piceapollenites*, *Podocarpidites*, *Pristinuspollenites*; 8: *Araucariacites*, *Balmeiopsis*, *Calliallasporites*; 9: *Classopollis*; 10: *Exesipollenites*, *Inaperturopollenites*, *Perinopollenites*, *Taxodiaceapollenites*; 11: *Alisporites*, *Afropollis*, *Cycadopites*, *Eucommiidites*, *Monosulcites*; 12: *Clavatipollenites*, *Dichastopollenites*, *Pennipollis*, *Retimonocolpites*, *Stellatopollis*, *Transitoripollis*; 13: *Artiopollis*, *Nyssapollenites*, *Phimopollenites*, *Retitrescolpites*, *Tricolpites*. Species list, counts and references are available on Appendix S1. B–Z. Dinocysts, spores and pollen grains recovered from Neau lignitic clays. Accompanying data are palynological preparation and England Finder coordinates. Scale bars represent 10  $\mu$ m. B. *Surculosphaeridium longifurcatum* (Firtion) Davey *et al.*, S3-Cd9, N30.4. C. *Triporoletes cenomanianus* (Agasie) Srivastava, S11-Cd28, R45.4. D. *Camarozonosporites insignis* Norris, S4-Cd16, J31.4. E. *Cicatricosisporites* cf. *mohrioides* Delcourt and Sprumont, S11-Cd31, P36.0. F. *Cicatricosisporites annulatus* Archangelsky and Gamarro, S3-Cd9, F29.2. G, H. *Appendicisporites bilateralis* Singh, S3-Cd7, K41.0. I, J. *Appendicisporites insignis* (Markova) Chlonova, S4-Cd11, J46.1. K. *Baculatisporites* sp., S3-Cd8, R48.1. L. *Patellasporites tavadensis* Groot and Groot, S11-Cd28, J42.0. M. *Podocarpidites biformis* Rouse, S3-Cd6, M32.3. N. *Araucariacites australis* Cookson ex Cooper, S11-Cd31, L47.1. O. *Eucommiidites minor* Groot and Penny, S11-Cd29, P45.0. P. *Transitoripollis anulisulcatus* Góczán and Juhász, S3-Cd6, M31.0. Q. *Dichastopollenites reticulatus* May, S4-Cd14, S46.4. R. *Dichastopollenites* sp. 4 *sensu* Heimhofer *et al.*, (2007), S11-Cd29, B40.0. S. *Stellatopollis* cf. *largissimus* Singh, S4-Cd16, K48.0. T. *Artiopollis indivisus* Agasie, S4-Cd16, K52.1. U. *Nyssapollenites albertensis* Singh, S3-Cd8, R48.3. V. *Tricolpites* cf. *vulgaris* (Pierce) Srivastava, S3-Cd7, H48.4. W. *Tricolpites* aff. *virgeus* (Groot, Penny and Groot) Hasenboehler, S11-Cd28, F35.0. X. *Phimopollenites tectatus* Singh, S3-Cd7, K47.1. Y. *Phimopollenites megistus* Singh, S4-Cd16, M33.1. Z. *Phimopollenites* cf. *pannosus* (Dettmann and Playford) Dettmann, S11-Cd33, L37.4.

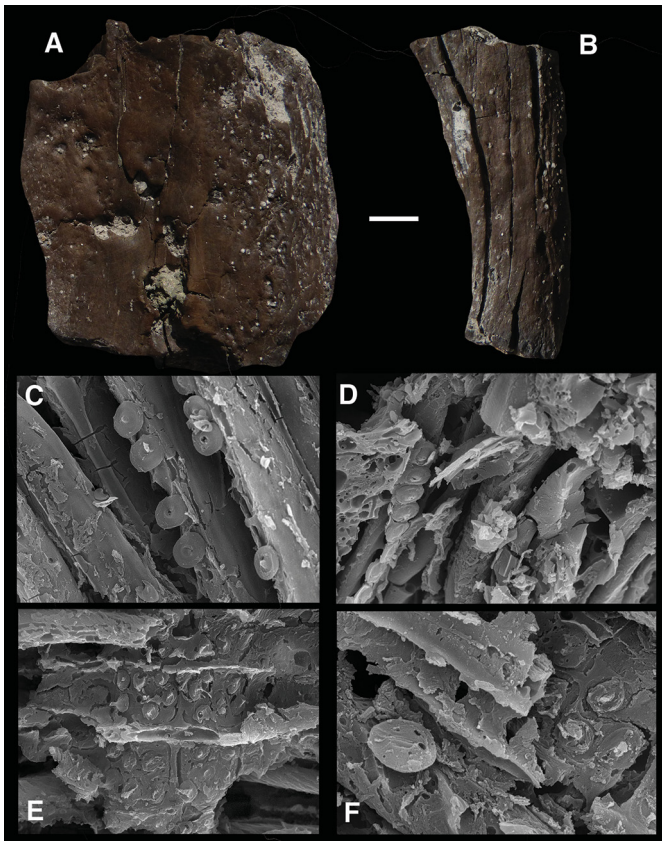


**Fig. 9.** Optical (A–B) and SEM (C–F) photographs of wood fragments. A. Large piece of fossil wood showing large *Teredo* borings on the left and numerous tiny borings (insect attacks?) on the right, IGR-PAL-2828. B. Piece of branch showing tiny borings IGR-PAL-2829. C. Areolated pit inner casts; note that tori left a circular depression in the centre of the casts (magnification  $\times 1700$ ). D. Araucarian row of uniseriate contiguous radial pits (magnification  $\times 1300$ ). E. Five araucarioid cross-fields, with poorly preserved contiguous alternate cupressoid oculipores (magnification  $\times 1600$ ). F. An isolated areolated pit (foreground) and an araucarioid cross-field (background) (magnification  $\times 3500$ ). SEM observations have been made on specimen IGR-PAL-2846. Scale bar for A and B: 10 mm.

creating this new form only to accommodate Cenomanian French pollen grains. *Classopollis tenuiparietalis* is thus considered invalid. As the morphological differences between *C. obidosensis*, *C. classoides* Pflug, and *C. torosus* (Reisinger), Couper are very tenuous, we consider them all synonymous of the first form described, *Classopollis torosus* (see diagnoses of Couper, 1958, pp. 156–157, and Groot and Groot, 1962, p. 161). This latter species is then adopted for the pollen grains from Neau amber.

Trapped palynomorphs have been mostly recovered from Eocene Baltic amber (Wetzel, 1953; Arnold, 1998; see Langenheim and Bartlett, 1971 for 1800s and early 1900s references). A few other studies on subsidiary Cenozoic amber bearing strata have also documented spores and pollen grains in Eocene amber from France (Breton *et al.*, 1999; De Franceschi *et al.*, 2000; Dejax *et al.*, 2001), and Miocene amber from Peru and Mexico (Langenheim in Poinar, 1992, p. 78; Antoine *et al.*, 2006). Mesozoic records are scarce, and

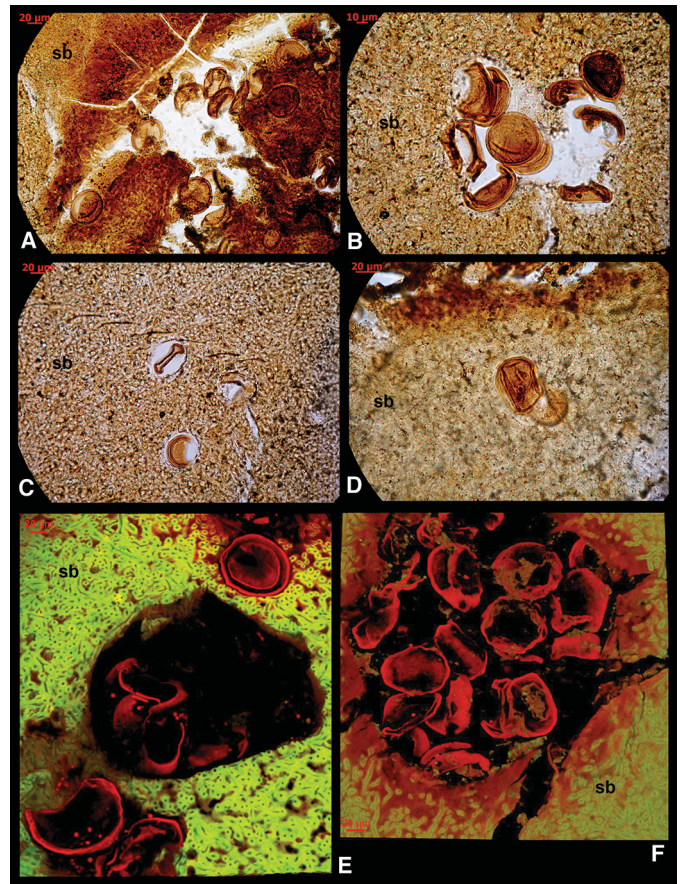


**Fig. 10.** Palynomorphs inclusions in amber. A–F. Inclusions of *Classopollis* pollen grains in the Cenomanian amber of Neau (Mayenne). Generally pollen grains are grouped in vacuoles of the amber and can be numerous (A, B, E, F), IGR-PAL-2837 to IGR-PAL-2840. Only a few ones are isolated in the fossil resin (C, D), IGR-PAL-2841 and IGR-PAL-2842. Note the dense filamentous network due to the colonization of the resin by a sheathed bacterium (sb). A–D. Optical microscope. E–F. Confocal microscope (CLSM).

concerns exclusively Cretaceous strata. Angiospermous pollen grains and spores were apparently recovered from Lower Cretaceous Lebanese amber, but neither precise reference nor illustrations are provided (Azar *et al.*, 2010; Engel *et al.*, 2011; Whalley in Poinar, 1992, p. 161). Several clusters of gymnosperm and angiosperm pollen grains were recovered from the Cenomanian Myanmar amber, always observed in association with various insects (Poinar, 2010; Cai *et al.*, 2018; Grimaldi *et al.*, 2019; Lin *et al.*, 2019; Hinkelman and Vrřanská, 2020). In Europe, *Monsulcites* grains were observed within late Albian amber from Spain (Peris *et al.*, 2017). The *Classopollis* clusters described herein are the first pollen grains documented from Mesozoic French amber so far.

#### 4.2.3 Microinclusions

The amber of Neau contains various inclusions of microorganisms (Saint Martin *et al.*, under study) characterized by centripetal colonization of filamentous networks. They are essentially sheathed bacteria identifiable as *Leptotrichites resinatus* Schmidt 2005 whose colonization density in the

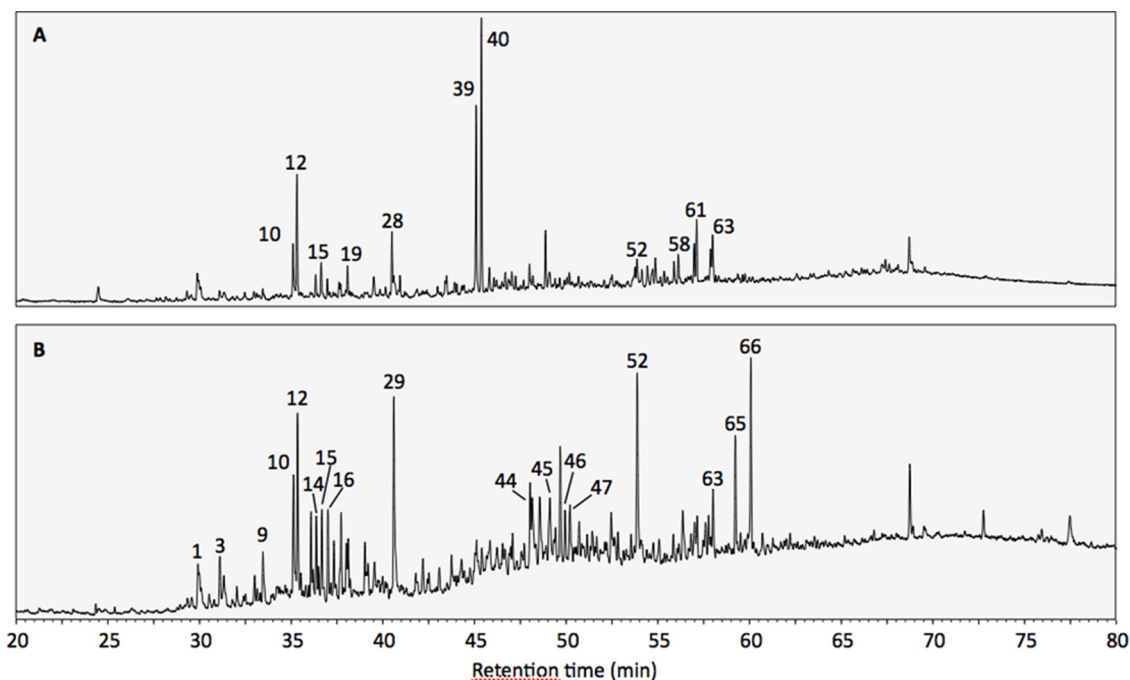


**Fig. 11.** Total ion chromatogram from the THM-GC-MS analysis of Neau amber form A (A) and form B (B). Numbered peaks refer to identified compounds in Table 1 and Appendix S2.

**Table 2.** Relative proportions of the three categories of identified compounds and of labdanoid diterpenes. Compositional ratio calculated on the distribution of labdanoid diterpenes.

	Form A	Form B
<i>Relative proportions of identified compounds</i>		
Labdanoid diterpenes	64	20
Methyl(hydro)naphthalene and methylphenanthrene <sup>a</sup>	21	64
Tricyclic diterpenes	15	16
<i>Relative proportions of labdanoid diterpenes</i>		
Carboxylic acid	66	11
Alcohol	8	15
1-Dimethyl	3	12
1-Methyl	23	62
<i>Compositional ratios <math>\Sigma C_{14}/\Sigma C_{15}</math></i>		
Carboxylic acid	0.23	0.11
Alcohol	0.22	0.09
1-Dimethyl	0.77	0.34
1-Methyl	0.71	0.88
All labdanoid diterpenes	0.24	0.17

<sup>a</sup> Including amberene.

initial resin results of the complete opacification of the amber grains (Figs. 7C, D, 8E, I, 10A–F), and often of black colouring of the peripheral parts of the amber drops, just below the crust surface (Fig. 7D). These microinclusions are very widespread in Cretaceous ambers (Schmidt and Schäfer, 2005; Saint Martin and Saint Martin, 2018). Smaller clumps of

actinomycetes are also found to a lesser extent, located on the periphery of the amber grains.

#### 4.2.4 Chemical characteristics

The total ion chromatograms of the THM-GC-MS analysis of the Neau resins are illustrated in Figure 11. The relative proportions of (i) the different categories of compounds and (ii) labdanoid diterpenes and compositional ratios are given in Table 2. The molecular fingerprint was composed of 66 molecules from three main families: (i) labdanoid diterpenes produced by the thermochemolysis of the A/B ring system of a polylabdanoid structure, (ii) methyl(hydro)naphthalene and methylphenanthrene and (iii) tricyclic diterpenes. Both pieces of ambers produced a different chemical fingerprint. Most of the compounds (80%) occurred in both fingerprints, but in different relative proportions.

Labdanoid diterpenes are the main chemical group in form A (64% of the analyzed compounds), while they only represent 20% of the analyzed compounds in form B (Tab. 2). The similarity of the retention times of the carboxylic acids compared with Baltic amber and the absence of dimethyl succinate classified these samples as Class Ib ambers. Labdanoid diterpens of form A are dominated by bicyclic acids (66%) with a large predominance of C<sub>15</sub> over C<sub>14</sub> ( $\Sigma C_{14}/\Sigma C_{15}=0.23$ ). In form B, they are dominated by 1-methyl-bicyclic hydrocarbons (64% of labdanoid diterpens) with a slight predominance of C<sub>15</sub> over C<sub>14</sub> ( $\Sigma C_{14}/\Sigma C_{15}=0.88$ ).

Methyl(hydro)naphthalene and methylphenanthrene are the main chemical group in form B (64% of analyzed compounds), while they represent 21% of the analyzed compounds in form A. This group included trimethylindene, ionene, methylionene and diagenetic products of sesqui- and diterpenoids. The distribution of these compounds is quite

similar in both form with the predominance of 5 isomers of trimethylnaphthalene (38 and 36% in form A and B, respectively) and 2 isomers of dimethylnaphthalene (17 and 13% in form A and B, respectively). Amberene was detected in low amount in the program of form B and represented 0.5% of this chemical group.

The third chemical category was composed of tricyclic diterpenes. In form A, this group was dominated by methyl 16,17-dinordehydroabietate (23%), dimethylphenanthrene (19%) and methyl 8-abieten-18-oate (15%) with low occurrence of callitrisic acid derivatives. In form B, this group was dominated by dimethylphenanthrene (32%), methyl dehydroabietate (13%) and the isomers of trimethylphenanthrene (12%). Methyl callitrisate (5% and methyl 16,17-dinorcallitrisate (1%) were also detected.

## 5 Discussion

### 5.1 Singularity of the amber from Neau

The appearance of the Cenomanian amber of Neau is very similar to that of the amber grains generally collected in many Cretaceous French amber deposits of various ages. The same reduced size and the drop shape of the best preserved grains can be found in other Cenomanian French sites: *e.g.* Poitou (Valentin *et al.*, this volume), Sarthe (Breton and Tostain, 2005; Breton, 2007; Girard *et al.*, 2013a, 2013b). This feature is also common for the Turonian of Dordogne (Saint Martin *et al.*, 2013a, 2013b; Néraudeau *et al.*, 2016) and Aude (Breton *et al.*, 2018), the Santonian of Provence (Saint Martin *et al.*, 2012, 2013; Saint Martin and Saint Martin, 2018; Frau *et al.*, this volume; Saint Martin *et al.*, this volume), and the Campanian of Aude (Breton *et al.*, 2013). On the other hand, they do not correspond to amber samples taken from the Albo-Cenomanian of Charente Maritime or the Upper Cretaceous from Vendée, where large nodules can be found (Néraudeau *et al.*, 2008; Girard, 2010; Néraudeau *et al.*, 2017).

Consequently, like in Dordogne, Poitou or Provence ambers, the very small size of the amber drops from Neau did not favour the preservation of arthropod inclusions as large amber drops from the Charentes and Vendée did. The only micro-inclusions that have been observed in the amber from Neau correspond to filamentous organisms such as sheathed bacteria and actinomycetes. But other micro-organisms, such as amoeba or diatoms seem to be lacking.

Conversely, palynological inclusions, which were never observed in French Cretaceous ambers, are well preserved in Neau amber (see Sect. 4.2.2). The lack of palynomorphs, known to be resistant to physical and chemical taphonomical processes, is difficult to explain for the other Cretaceous French ambers. Their presence in the Mayenne amber could be related to a season of resin flow more contemporaneous to the conifer pollination. Langenheim and Bartlett (1971) have noticed that the probability of finding pollen in amber can be increased when pollen was produced throughout the entire period of resin secretion. However, they also observed that several genera of palynomorphs were trapped throughout the year within resin, regardless of either time of pollination and period of resin production. As Cretaceous palynomorphs have been generally noticed when they are found in association with insects and plants (see Sect. 4.2.2), it could be possible that

spores and pollen grains were trapped within other Cretaceous amber, but were not observed because they were not in the vicinity of larger fossils. However, the researches of Girard (2010), (2013, 2018) and Saint Martin *et al.* (2012, 2013a, 2013b) dedicated to the identification of every micro-inclusions in French Cretaceous ambers devoid of arthropod inclusions, have never observed pollen grains in these ambers, in spite of their diversity of geographical (centre-western, south-western or south-eastern France) and stratigraphical (Albian, Cenomanian, Turonian, Santonian, Campanian) origins. The case of Lebanese amber shows another original situation, the pollen grain species trapped in the Lower Cretaceous Hammana amber lacking in the palynological assemblage of the sediment containing the amber (Azar *et al.*, 2010).

The chemical fingerprints of form A and B ambers composed of labdanoid diterpenes produced, methyl(hydro)naphthalene, methylphenanthrene and tricyclic diterpenes is typical of Cretaceous ambers (Anderson, 2006; Bray and Anderson, 2008; Menor-Salván *et al.*, 2016; Nohra *et al.*, 2015). Both chemical fingerprints shared 80% of the detected compounds and the 66 analyzed molecules fall in the three aforesaid chemical classes. Based on the higher proportion of methyl (hydro)naphthalene and methylphenanthrene (Clifford *et al.*, 1995) and lower  $\Sigma C_{14}/\Sigma C_{15}$  (Clifford *et al.*, 1999), the differences in the chemical fingerprints could be interpreted as a higher degree of maturation for form B than for form A. However both come from the same deposit, so the same diagenetic conditions could be assumed. Since 80% of the molecules are common to both fingerprints, a similar botanical precursor may be assumed. In such a situation, the differences between both fingerprints could be due to the initial composition of the resin that can present large seasonal and inter-specific variations (Langenheim, 2003) and/or from heterogeneities in the physico-chemical conditions of the deposit.

The chemical fingerprint of form A is characterized by (i) the predominance of labdanoid diterpenes with a predominance of bicyclic acids and (ii) the occurrence of tricyclic diterpenes coming from dehydroabietic and callitrisic acids with a predominance of dehydroabietic acid derivatives. It is similar to that described for the Cretaceous amber from the Raritan formation (Anderson, 2006) that has been assigned to the Cupressaceae. However the vegetal macrofossils from Neau are not from this family. Moreover the chemical fingerprint of the Cretaceous amber from Vendée (France) assigned to the Cupressaceae is characterized by a large predominance of callitrisic acid derivatives over dehydroabietic acid derivatives (Nohra *et al.*, 2015).

Bisnorsimonellite also occurred in form A. The chemical fingerprint of this form A is similar to that described for the Charentese (France) Cretaceous amber (Nohra *et al.*, 2015). The chemical fingerprint of the form B is characterized by the occurrence of traces of amberene and by a higher proportion of 16,17,18-trisnorabieta-8,11,13-triene *versus* 18-norabieta-triene. It is similar to that described for the type 2 Cretaceous ambers from Spain (Menor-Salván *et al.*, 2016). The extinct family Cheirolepidiaceae has been suggested as the potential producer of these ambers, which is in accordance with the vegetal macrofossils associated with the Neau ambers. Consequently Neau ambers may be assigned to the Cheirolepidiaceae.

The present data reinforce the chemical signature suggested for the ambers produced by the extinct family Cheirolepidiaceae. The combination of previous observations (Bray and Anderson, 2008; Menor-Salván *et al.*, 2016; Nohra *et al.*, 2015) and the present data suggests the following chemical fingerprint: (i) occurrence of labdanoid diterpenes, (ii) occurrence of tricyclic diterpenes coming from dehydroabietic and callitrisic acids with a predominance of dehydroabietic acid derivatives, (iii) a higher proportion of 16,17,18-trisnorabieta-8,11,13-triene *versus* 18-norabieta-triene (Tab. 2), (iv) absence or occurrence in low proportion of amberene and (v) occurrence of ferruginol or its diagenetic products such as bisnorsimonellite.

## 5.2 Age of the lignitic clay(s)

Despite the revealing title of their study, Azema *et al.* (1972) did not consider all the palynological assemblages they observed to be mid-Cenomanian in age. This is the case of the palynoflora recovered from Neau, which they interpreted as lower to mid Cenomanian. They based their age attribution (1) on the presence of the same species of *Classopollis* in the clays of both Neau and Ecommoy, the latter being unequivocally mid-Cenomanian, and (2) on the absence of the form *Lobelina*, which would be indicative of an Albian age (Azema *et al.*, 1972, p. 10). However, we consider herein that the specimens identified as *Classopollis* belong to the long-ranging form *C. torosus* (see Sect. 3.2). Moreover, the Circumpolle genus *Lobelina* created by Médus (1970) was later proven to be a *nomen nudum* (Jansonius and Hills, 1976), and is considered as a form of *Classopollis*. In any case, the use of Circumpolles to date Mesozoic deposits has not been proven satisfactory in spite of Médus efforts to produce a comprehensive morphologic and stratigraphic identification key (Médus, 1970). Thus, to confirm the age attribution made by Azema *et al.* (1972), supplementary palynological arguments must be made.

Several observations support a Cenomanian rather than Albian age for the lignitic clays of Neau. The presence of *Artiopollis indivisus* (Fig. 6T) is worth being noted, this form having been observed only in Late Cretaceous palynofloras so far, especially Cenomanian (Singh, 1983; Ravn and Witzke, 1995; Lupia, 1999). The occurring of *Microreticulatisporites sacalii* is sometime considered as a stratigraphic argument in favour of a Cenomanian age (Peyrot *et al.*, 2019) because it has been almost exclusively found within Cenomanian strata (Deák and Combaz, 1967; Médus and Triat, 1969; Peyrot *et al.*, 2019), but Ravn (1995) observed this species in late Albian assemblages of Wyoming. If this form is frequently encountered, it may be considered as relatively stratigraphically significant, when coupled with other stratigraphic arguments. The observation of numerous tricolpoidate and tricolporate forms, such as *Phimopollenites* and *Nyssapollenites*, is also indicative of Cenomanian rather than Albian assemblages. Specimens belonging to those genera, and more generally tricolporate pollen grains, appear very scarcely during the Albian, but become much more frequent and diverse during the Cenomanian (Doyle and Robbins, 1977; Hochuli *et al.*, 2006). Actually, those tricolpoidate and tricolporate specimens were encountered more frequently in the palynoflora from Neau than in the lower Cenomanian palynofloras recovered from

Charente-Maritime, Charente, and Vienne (Peyrot *et al.*, 2019; Polette *et al.*, 2019). The absence of indubitable mid-Cenomanian markers, such as Normapolles, has to be acknowledged. The lack of observation does not necessarily mean that Normapolle grains were not present in Neau palynoflora, and the absence of a form cannot be considered as stratigraphically significant. However, Normapolles complex diversified quite rapidly from the end of mid Cenomanian onward (Méon *et al.*, 2004) and several species were usually encountered from other mid to late Cenomanian assemblages from western France (Azema *et al.*, 1972; Néraudeau *et al.*, 2017). If they were to be found in Neau lignites, they are certainly very scarce.

The palynoflora from Neau is then probably younger than the charentese palynofloras, and older than Normapolles-rich mid Cenomanian palynofloras from Vendée (western France; Azema *et al.*, 1972; Néraudeau *et al.*, 2017), agreeing with the regional stratigraphic correlations of Azema *et al.* (1972). A possible age of upper lower Cenomanian or lower mid Cenomanian (which is virtually the same) is then attributed to the Neau amber-bearing lignitic clays.

## 5.3 Palaeoenvironment

Such poorly diversified conifer-dominated plant assemblage is common in the Laurasian littoral floras during the Albian-Cenomanian. Albian-Cenomanian floras yielding the conifer *Frenelopsis* as well as the ginkgophyte *Eretmophyllum* (or *Nehvizdya*) were reported from several palaeobotanical sites of western France, including the Archingey quarry and the Renardières quarry in Charente-Maritime (Néraudeau *et al.*, 2005), and the Brouillard quarry in Maine-et-Loire (Pons, 1979; Néraudeau *et al.*, 2013). The abundance of both the leafy axis *Frenelopsis* and the dispersed pollen grain *Classopollis* as well as the chemical signature of the amber suggest that Cheirolepidiaceae were one of the main components of the flora bordering the palaeokarsts from Neau. Although both are isolated in the sediment from Neau, *Classopollis* was reported attached on microsporangiote cones of *Frenelopsis alata* from other Cenomanian palaeobotanical sites of Europe (e.g. Kvaček, 2000). As it was remonstrated in the Albian-Cenomanian deposits of western France (e.g. Pons, 1979; Néraudeau *et al.*, 2005, 2013; Girard *et al.*, 2013a, 2013b; Moreau *et al.*, 2014, 2017) and other European localities (e.g. Kvaček, 2000), the genus *Frenelopsis* is related to littoral environments commonly with strong marine influence. Ecophysiologicaly, the xerophytic characters of the conifer *Frenelopsis* clearly show that the flora from Neau was adapted to withstand intense sunlight and coastal environments exposed to desiccant conditions coupled in haline settings: sheathing leaves, thick cuticle, grooved epidermal cells, epidermal hairs, stomata in sunken lines, and stomata with two levels of papillae (Thévenard *et al.*, 2005). These morphoanatomical characteristics allow a reduction of solar radiations, drying air circulations and evapotranspiration.

*Classopollis* shows a wide geographical distribution. The genus has been reported in high proportions from near-coastal settings, such as sandy bars or coastal islands with well-drained soils (Alvin, 1982; Abbink, 1998), as well as in upland

slope habitats (Filatoff, 1975; Vakhrameev and Doludenko, 1977). However, the abundance of *Classopollis* in the Jurassic and Cretaceous of Russia and North America shows a marked decrease northward, at higher and cooler palaeolatitudes (Pocock, 1972). When recovered with *Frenelopsis* remains, the presence of this genus is likely to be indicative of warm coastal habitats. The observation of numerous *Classopollis* clusters within the amber from Neau suggests that their parent plants grew in the vicinity of the depositional environment. The presence of very scarce *Surculosphaeridium longifurcatum* and foraminifera lining supports the hypothesis of an environment submitted to occasional marine inputs (Appendix S1; Fig. 6A).

The composition of the palynological assemblages of Neau is very similar to that of the Cenomanian assemblages from western France described by Peyrot *et al.* (2019) and Polette *et al.* (2019), sharing numerous common species. The present study underlines the fact that all lower to mid-Cenomanian spore assemblages from western France are dominated by Anemiaceae, Gleicheniaceae, and Cyatheales, with often numerous lycopods, mostly belonging to *Camarozonosporites* (see Azema *et al.*, 1972; Peyrot *et al.*, 2019; Polette *et al.*, 2019). Modern Cyatheales are concentrated at the tropics but can occupy varied habitats (Kramer in Kramer and Green, 1990). Their recurring presence at Neau agrees with a globally warm mid-Cretaceous climate, already suggested by the numerous *Classopollis* pollen grains (Kujau *et al.*, 2013). Representatives of the Gleicheniaceae are considered to be opportunistic, pioneering tropical to subtropical plants, adapted to long droughts, growing in unstable habitats such as dry forests and wetlands that occasionally dry out (Coiffard *et al.*, 2007; Mehlreter *et al.*, 2012; Kujau *et al.*, 2013). Modern Anemiaceae usually develop under warm and humid environments, and their Mesozoic relatives may have grown along riverbanks, or as understorey in forests (Dettmann and Clifford, 1991; Van Konijnenburg-Van Cittert, 2002). However, some species of Anemiaceae are adapted to more arid conditions, and may tolerate partial desiccation (Proctor and Tuba, 2002; Schrank, 2010). No suggestion has been previously made about the ecological requirements of the potential parent plant of *Camarozonosporites*, which has been associated with Lycopodiaceae (Ravn, 1995; Schrank, 2010). Extant forms usually develop in fairly sheltered, dark and humid environments, such as conifer forests understorey. They also can grow along riverbanks and streams, or as epiphytes on mossy tree trunks (Rusea *et al.*, 2009). A few species, such as *Lycopodiella cernua*, are even adapted to more arid condition, and can develop in open and sunny areas (Rusea *et al.*, 2009). While some representatives of Gleicheniaceae, Anemiaceae, and Lycopodiaceae correspond to drought-resistant plants, the majority of extant ferns flourishes in wet conditions, and a high spore content is generally used as indicator of humid settings. Subordinate elements of the palynoflora, such as *Todisporites*, or diversified Eudicots pollen assemblage support the hypothesis of the existence of a partly riparian hygrophilous plant community (Abbink *et al.*, 2004; Peyrot *et al.*, 2019). Other minor forms recovered from Neau palynoflora, such as *Densoisporites* and *Alisporites*, have been interpreted as indicators of tidally influenced environments (Abbink *et al.*, 2004). The recurring presence of several species of cupressaceous inaperturate pollen

grains herein, including *Inaperturopollenites dubius*, *Taxodiaceapollenites hiatus*, *Perinopollenites halonatus*, along with araucariaceous related forms (Appendix S1) could also suggest also the existence of conifer forests linked to wet lowlands, such as in low salinity back-swamp environments, based on the ecological requirement of some modern Cupressaceae (Schrank, 2010; Peyrot *et al.*, 2019; Appendix S1).

Peyrot *et al.* (2019) and Polette *et al.* (2019) discussed extensively the hypothetical environmental settings corresponding to Cenomanian palynofloras from western France, and described various riparian to coastal plant communities which developed under humid and warm condition. They are associated with palynological assemblages grading from (1) assemblages clearly dominated by *Classopollis* which would indicate downstream and coastal environments associated with xeric communities (cheirolepids, some representatives of drought-tolerant Gleicheniaceae and Anemiaceae) to (2) assemblages dominated by diversified spores, bisaccates and angiosperm pollen grains which would represent more upstream depositional environments associated with riparian hygrophilous plant communities. The composition of the palaeobotanical and palynological assemblages from Neau is intermediate. The corresponding depositional environment was subjected to a very limited connection to the sea, while associated with both drought-resistant plants and hygrophilous ferns and angiosperms. It could well have corresponded to the upstream portion of a mangrove or the most inner part of a lagoon. Depositional settings associated with mangrove-type environments has now been abundantly suggested to accommodate lower to mid-Cenomanian plant communities of western Europe (Batten, 1974; Gomez *et al.*, 2008; Peyrot *et al.*, 2019; Polette *et al.*, 2019). The abrupt increase of the abundance of angiosperm pollen grains is interpreted as a reflection of the group's radiation.

## Supplementary Material

**Appendix S1.** Species list of palynomorphs recovered from the productive lower mid-Cenomanian clay deposits of Neau, along with potential botanical affinities and counts per sample.  
**Appendix S2.** Molecules identified in the pyrolysates of Neau ambers. Individual compounds are labelled according to the identification of peaks in Table 1.

The Supplementary Material is available at <https://www.bsgf.fr/10.1051/bsgf/2020039/olm>.

**Acknowledgements.** The authors are greatly indebted to the *Société Chaux & Dolomie Françaises/Lhoist France Ouest* for the authorization to access to the outcrop. They thank Paul Bessin and Valentin Prugneaux for their participation to the field trip. The preparation of thin sections was performed by Severin Morel (UMR 7207). We thank also Géraldine Toutirais (PTME, Muséum National d'Histoire Naturelle, Paris) for his assistance with scanning electron microscopy. The CLSM investigations were performed at the Institute of Biology Paris-Seine Imaging Facility that is strongly supported by the "Conseil Régional Île-de France", the French National Research Council (CNRS) and Sorbonne University.

## References

- Abbink OA. 1998. Palynological investigations in the Jurassic of the North Sea region. In: *LPP Contribution Series 8*. Utrecht: University of Utrecht, 192 p.
- Abbink OA, Van Konijnenburg-Van Cittert JHA, Visscher H. 2004. A sporomorph ecogroup model for the Northwest European Jurassic-Lower Cretaceous: concept and framework. *Netherlands Journal of Geosciences* 83: 17–38.
- Aimin F, Xiaohan L, Weiming W, Xiaoli L, Liangjun Y, Feixin H. 2005. Preliminary study on the spore-pollen assemblages found in the Cenozoic sedimentary rocks in Grove Mountains, east Antarctica and its climatic implications. *Chinese Journal of Polar Sciences* 16: 23–32.
- Alvin KL. 1982. Cheirolepidiaceae: biology, structure and paleoecology. *Review of Palaeobotany and Palynology* 37: 71–98.
- Anderson KB. 1994. The nature and fate of natural resins in the geosphere—IV. Middle and Upper Cretaceous amber from the Taimyr Peninsula, Siberia—evidence for a new form of polyabdanoid of resinite and revision of the classification of Class I resinites. *Organic Geochemistry* 21(2): 209–212. [https://doi.org/10.1016/0146-6380\(94\)90155-4](https://doi.org/10.1016/0146-6380(94)90155-4).
- Anderson KB. 1996. New evidence concerning the structure, composition, and maturation of class I (Polyabdanoid) resinites. In: *Amber, Resinite, and Fossil Resins*. American Chemical Society 617: 105–129.
- Anderson KB. 2006. The nature and fate of natural resins in the geosphere. XII. Investigation of C-ring aromatic diterpenoids in Raritan amber by pyrolysis-GC-matrix isolation FTIR-MS. *Geochemical Transactions* 7(2). <https://doi.org/10.1186/1467-4866-7-2>.
- Antoine P-O, De Franceschi D, Flynn JJ, Nel A, Baby P, Benammi M, *et al.* 2006. Amber from western Amazonia reveals Neotropical diversity during the middle Miocene. *Proceedings of the National Academy of Sciences* 103: 13595–13600.
- Archangel'sky S, Archangel'sky A. 2005. *Aequitriradites* Delcourt & Sprumont y *Couperisporites* Pocock, esporas de hepáticas, en el Cretácico Temprano de Paragonia, Argentina. *Revista del Museo Argentino de Ciencias Naturales* 7: 119–138.
- Arnold V. 1998. Vergessene Einschlüsse-Blütenstaub in baltischem Bernstein. *Mitteilungen aus dem Geologisch-Paläontologischen Institut. Univ. Hamburg* 81: 269–282.
- Azar D, Gèze R, Acra F. 2010. Lebanese amber. In: Penney D, ed. *Biodiversity of fossils in amber from the major world deposits*. Manchester (UK): Siri Scientific Press, pp. 271–298.
- Azema C, Durand S, Medus J. 1972. Des miospores du Cénomaniens moyen. *Paléobiologie continentale, Montpellier, France* 3: 1–54.
- Balme BE. 1995. Fossil *in situ* spores and pollen grains: an annotated catalogue. *Review of Palaeobotany and Palynology* 87: 81–323.
- Batten DJ. 1974. Wealden palaeoecology from the distribution of plant fossils. *Proceedings of the Geologists' Association* 85: 433–457.
- Batten DJ, Dutta RJ. 1997. Ultrastructure of exine of gymnospermous pollen grains from Jurassic and basal Cretaceous deposits in Northwest Europe and implications for botanical relationships. *Review of Palaeobotany and Palynology* 99: 25–54.
- Bray PS, Anderson KB. 2008. The nature and fate of natural resins in the geosphere XIII: a probable pinaceous resin from the early Cretaceous (Barremian), Isle of Wight. *Geochemical Transactions* 9(3). <https://doi.org/10.1186/1467-4866-9-3>.
- Breton G. 2007. La bioaccumulation de microorganismes dans l'ambre : analyse comparée d'un ambre cénomaniens et d'un ambre sparnacien, et de leurs tapis algaires et bactériens. *Comptes Rendus Palevol* 6: 125–133.
- Breton G, Gauthier C, Vizcaïno D. 1999. Land and freshwater microflora in a Sparnacian amber from the Corbières (South France): first observations. *Estudios del Museo de Ciencias Naturales de Álava* 14: 161–166.
- Breton G, Bilote M, Eychenne G. 2013. L'ambre campanien du Mas d'Azil (Ariège, France) : gisement, microinclusions, taphonomie. *Annales de paléontologie* 99: 317–337.
- Breton G, Champion S, Bilote M. 2018. L'ambre turonien du ruisseau des Tarquès (Commune de Duilhac-sous-Peyrepertuse, Aude, France). *Bulletin de la Société d'Histoire Naturelle de Toulouse* 154: 161–176.
- Breton G, Tostain F. 2005. Les microorganismes de l'ambre cénomaniens d'Ecommoy (Sarthe, France). *Comptes Rendus Palevol* 4: 31–46.
- Cai C, Escolana HE, Li L, Yin Z, Huang D, Engel MS. 2018. Beetle Pollination of Cycads in the Mesozoic. *Current Biology* 28: 2806–2812.
- Clifford DJ, Carson DM, McKinney DE, Bortiatynski JM, Hatcher PG. 1995. A new rapid technique for the characterization of lignin in vascular plants: thermochemolysis with tetramethylammonium hydroxide (TMAH). *Organic Geochemistry* 23(2): 169–175. [https://doi.org/10.1016/0146-6380\(94\)00109-E](https://doi.org/10.1016/0146-6380(94)00109-E).
- Clifford DJ, Hatcher PG, Botto RE, Muntean JV, Anderson KB. 1999. The nature and fate of natural resins in the geosphere. IX Structure and maturation similarities of soluble and insoluble polyabdanoids isolated from Tertiary Class I resinites. *Organic Geochemistry* 30 (7): 635–650. [https://doi.org/10.1016/S0146-6380\(99\)00018-2](https://doi.org/10.1016/S0146-6380(99)00018-2).
- Coiffard C, Gomez B, Thévenard F. 2007. Early Cretaceous angiosperm invasion of Western Europe and major environmental changes. *Annals of Botany* 100: 545–553.
- Collectif. 2010. Histoire géologique de la Mayenne. Épisode 5 : Mésozoïque. Éditions Errance, pp. 245–248.
- Couper RA. 1958. British Mesozoic microspores and pollen grains: a systematic and stratigraphic study. *Palaeontographica Abteilung B* 103: 75–179.
- De Franceschi D, Dejax J, De Ploëg G. 2000. Extraction du pollen inclus dans l'ambre [Sparnacien du Quesnoy (Oise), bassin de Paris] : vers une nouvelle spécialité de la paléo-palynologie. *Comptes rendus de l'Académie des sciences, de la terre et des planètes* 330: 227–233.
- Deák MH, Combaz A. 1967. « Microfossiles organiques » du Wealdien et du Cénomaniens dans un sondage de Charente-Maritime. *Revue de micropaléontologie* 10: 69–96.
- Dejax J, De Franceschi D, Lugardon B, De Ploëg G, Arnold V. 2001. Le contenu cellulaire du pollen fossilisé dans l'ambre, préservé à l'état organique. *Comptes rendus de l'Académie des sciences, de la terre et des planètes* 332: 339–344.
- Dettmann ME. 1963. Upper Mesozoic microfloras from southeastern Australia. *Proceedings of the Royal Society of Victoria* 77: 1–149.
- Dettmann ME, Clifford HT. 1991. Spore morphology of *Anemia*, *Mohria*, and *Ceratopteris* (Filicales). *American Journal of Botany* 78: 303–325.
- Doyle JA, Robbins EI. 1977. Angiosperm pollen zonation of the continental Cretaceous of the Atlantic coastal plain and its application to deep wells in the Salisbury Embayment. *Palynology* 1: 43–78.
- Doyle JA, Endress PK. 2018. Phylogenetic analyses of Cretaceous fossils related to Chloranthaceae and their evolutionary implications. *The Botanical Review* 84: 156–202.
- Durand S, Louail J. 1971. Découverte d'un dépôt cénomaniens fossilifère à Neau (Mayenne). *Comptes rendus de l'Académie des sciences de Paris* 273: 1179–1181.

- Dutta S, Mallick M, Kumar K, Mann U, Greenwood PF. 2011. Terpenoid composition and botanical affinity of Cretaceous resins from India and Myanmar. *International Journal of Coal Geology* 85(1): 49–55. <https://doi.org/10.1016/j.coal.2010.09.006>.
- Engel MS, Ortega-Blanco J, Azar D. 2011. The earliest earwigs in amber (Dermaptera): a new genus and species from the Early Cretaceous of Lebanon. *Insect Systematics and Evolution* 42: 139–148.
- Fensome RA. 1987. Taxonomy and biostratigraphy of schizaealean spores from the Jurassic-Cretaceous boundary beds of the Aklavik Range, District of Mackenzie. *Palaeontographica Canadiana* 4: 1–49.
- Filatoff J. 1975. Jurassic palynology of the Perth Basin, Western Australia. *Palaeontographica Abteilung B* 154: 1–113.
- Fleury R, Polette F, Batten DJ, Durand M, Moreau J-D, Néraudeau D, *et al.* 2017. Palaeobotanical investigation of a Cenomanian clay lens in Hucheloup quarry, Maine-et-Loire, NW France: taxonomic, stratigraphic and palaeoenvironmental implications. *Annales de paléontologie* 103: 235–250.
- Gingras MK, Maceacher JA, Picherill RK. 2004. Modern perspectives on *Teredolites* Ichnofacies: observations from Willapa Bay, Washington. *Palaos* 19: 79–98.
- Girard V. 2010. Microcénoses des ambres médio-crétaqués français. Taphonomie, systématique, paléoécologie et reconstitution du paléoenvironnement. *Mémoires Geosciences Rennes* 134: 1–294.
- Girard V, Néraudeau D, Breton G, Morel N. 2013a. Palaeoecology of the Cenomanian amber forest of Sarthe (western France). *Geologica Acta* 11: 321–330.
- Girard V, Breton G, Perrichot V, Bilotte M, Le Loeuff J, Nel A, *et al.* 2013b. The Cenomanian amber of Fourtou (Aude, Southern France): Taphonomy and palaeoecological implications. *Annales de paléontologie* 99: 301–315.
- Gomez B, Martín-Closas C, Barale G, Thévenard F. 2000. A new species of *Nehvizdya* (Ginkgoales) from the Lower Cretaceous of the Iberian Ranges (Spain). *Review of Palaeobotany and Palynology* 111: 49–70.
- Gomez B, Daviero-Gomez V, Perrichot V, Thévenard F, Coiffard C, Philippe M, *et al.* 2004. Assemblages floristiques de l'Albien-Cénomanien de Charente-Maritime (SO France). *Annales de paléontologie* 90: 147–159.
- Gomez B, Coiffard C, Dépré E, Daviero-Gomez V, Néraudeau D. 2008. Diversity and histology of a plant litter bed from the Cenomanian of Archingeay-Les Nouillers (southwestern France). *Comptes Rendus Palevol* 7: 135–144.
- Grimaldi DA, Peñalver E, Barrón E, Herhold HW, Engel MS. 2019. Direct evidence for eudicot pollen-feeding in a Cretaceous stinging wasp (Angiospermae; Hymenoptera, Aculeata) preserved in Burmese amber. *Communications Biology* 2: 1–10.
- Groot JJ, Groot CR. 1962. Plant microfossils from Aptian, Albian and Cenomanian deposits of Portugal. *Comunicações dos Serviços Geológicos de Portugal* 46: 133–176.
- Heimhofer U, Hochuli PA, Burla S, Weissart H. 2007. New records of Early Cretaceous angiosperm pollen from Portuguese coastal deposits: Implications for the timing of the early angiosperm radiation. *Review of Palaeobotany and Palynology* 144: 39–76.
- Hinkelman J, Vršanská L. 2020. A Myanmar amber cockroach with protruding feces contains pollen and a rich microcenosis. *The Science of Nature* 107: 19 p. (in press).
- Hochuli PA, Heimhofer U, Weissert H. 2006. Timing of early angiosperm radiation: recalibrating the classical succession. *Journal of the Geological Society, London* 163: 587–594.
- Jansonius J, Hills LV. 1976. Genera File of Fossil Spores and Pollen. 3287 cards. Special Publication. Calgary, Canada: Department of Geology, University of Calgary.
- Jiang Z, Philippe M, Zhang W, Tian N, Zheng S. 2016. A Jurassic wood that provides insights into the earliest steps in Ginkgo wood evolution. *Scientific Reports* 6: 38191. <https://doi.org/10.1038/srep38191>.
- Kramer KU, Green PS. 1990. The families and genera of vascular plants. I. Pteridophytes and Gymnosperms. Berlin: Springer-Verlag, 404 p.
- Kujau A, Heimhofer U, Hochuli PA, Pauly S, Morales C, Adatte T, *et al.* 2013. Reconstructing Valanginian (Early Cretaceous) mid-latitude vegetation and climate dynamics based on spore-pollen assemblages. *Review of Palaeobotany and Palynology* 197: 50–69.
- Kvaček J. 1999. New data and revision of three gymnosperms from the Cenomanian of Bohemia–*Sagenopteris variabilis* (Velenovský) Velenovský, *Mesenea bohémica* (Corda) comb. n. and *Eretmophyllum obtusum* (Velenovský) comb. n. *Acta Musei Nationalis Pragae, Series B, Historia Naturalis* 55: 15–24.
- Kvaček J. 2000. *Frenelopsis alata* and its microsporangiate and ovuliferous reproductive structures from the Cenomanian of Bohemia (Czech Republic, Central Europe). *Review of Palaeobotany and Palynology* 112: 51–78.
- Kvaček J, Falcon-Lang HJ, Dašková J. 2005. A new Late Cretaceous ginkgoalean reproductive structure *Nehvizdyella* gen. nov. from the Czech Republic and its whole-plant reconstruction. *American Journal of Botany* 92: 1958–1969.
- Kvaček J, Doyle P, Endress PK, Daviero-Gomez V, Gomez B, Tekleva M. 2016. *Pseudoasterophyllites cretaceus* from the Cenomanian (Cretaceous) of the Czech Republic: a possible link between Chloranthaceae and *Ceratophyllum*. *Taxon* 65: 1345–1373.
- Langenheim JH, Bartlett A. 1971. Interpretation of pollen in amber from a study of pollen in present-day coniferous resin. *Bulletin of the Torrey Botanical Club* 98: 127–139.
- Langenheim JH. 2003. Plant resins: chemistry, evolution, ecology, and ethnobotany. Portland, Oregon, USA: Timber Press.
- Lin X, Labandeira CC, Shih C, Hotton CL, Ren D. 2019. Life habits and evolutionary biology of new two-winged long-proboscid scorpion flies from mid-Cretaceous Myanmar amber. *Nature Communications* 10: 1–14.
- Lupia R. 1999. Discordant morphological disparity and taxonomic diversity during the Cretaceous angiosperm radiation: North American pollen record. *Paleobiology* 25: 1–28.
- May F. 1975. *Dichastopollenites reticulatus*, gen. et sp. nov.: potential Cenomanian Guide Fossil from Soutjern Utah and Northeastern Arizona. *Journal of Paleontology* 49: 528–533.
- Médus J. 1970. Contribution à la classification des grains de pollen du groupe des Circumpolles (Pflug) Klaus. *Pollen et Spores* 12: 205–216.
- Médus J, Triat J-M. 1969. Le Cénomanien supérieur de la coupe de Laudun (Gard, France) : étude palynologique et données sédimentologiques. *Review of Palaeobotany and Palynology* 9: 213–228.
- Mehlreter K, Walker LR, Sharpe JM. 2012. Fern ecology. Cambridge: Cambridge University Press.
- Menor-Salván C, Simoneit BRT, Ruiz-Bermejo M, Alonso J. 2016. The molecular composition of Cretaceous ambers: Identification and chemosystematic relevance of 1,6-dimethyl-5-alkyltetralins and related bisnorlabdane biomarkers. *Organic Geochemistry* 93: 7–21. <https://doi.org/10.1016/j.orggeochem.2015.12.010>.
- Méon H, Guignard G, Pacltová B, Svobodova M. 2004. Normapolles. Comparaison entre l'Europe centrale et du Sud-Est pendant le Cénomanien et le Turonien : évolution de la biodiversité et paléoenvironnement. *Bulletin de la Société géologique de France* 175: 579–594.
- Moreau J-D, Néraudeau D, Gomez B, Tafforeau P, Dépré E. 2014. Plant inclusions from the Cenomanian flints of Archingeay-Les Nouillers, western France. *Lethaia* 47: 313–322.

- Moreau J-D, Néraudeau D, Philippe M, Dépré E. 2017. Albien flora from Archingeay-Les Nouillers (Charente-Maritime): comparison and synthesis of Cretaceous meso- and macro-remains from the Aquitaine Basin (southwestern France). *Geodiversitas* 39: 729–740.
- Néraudeau D, Perrichot V, Dejax J, Masure E, Nel A, Philippe M, *et al.* 2002. Un nouveau gisement à ambre insectifère et à végétaux (Albien terminal probable) : Archingeay (Charente-Maritime, France). *Geobios* 35: 233–240.
- Néraudeau D, Allain R, Perrichot V, Videt B, De Broin F, Guillocheau F, *et al.* 2003. Découverte d'un dépôt paralic à bois fossiles, ambre insectifère et restes d'Iguanodontidae (Dinosauria, Ornithopoda) dans le Cénomanién inférieur de Fouras (Charente-Maritime, sud-ouest de la France). *Comptes Rendus Palevol* 2: 221–230.
- Néraudeau D, Vullo R, Gomez B, Perrichot V, Videt B. 2005. Stratigraphie et paléontologie (plantes, vertébrés) de la série margino-littorale Albien terminal – Cénomanién basal de Tonnay-Charente (Charente-Maritime, France). *Comptes Rendus Palevol* 4: 79–93.
- Néraudeau D, Perrichot V, Colin J-P, Girard V, Gomez B, Guillocheau F, *et al.* 2008. A new amber deposit from the Cretaceous (uppermost Albian-lowermost Cenomanian) of SW France. *Cretaceous Research* 29: 925–929.
- Néraudeau D, Vullo R, Gomez B, Girard V, Lak M, Videt B, *et al.* 2009. Amber, plant and vertebrate fossils from the Lower Cenomanian paralic facies of Aix Island (Charente-Maritime, SW France). *Geodiversitas* 31: 13–28.
- Néraudeau D, Redois F, Ballèvre M, Duplessis B, Girard V, Gomez B, *et al.* 2013. L'ambre cénomanién d'Anjou: stratigraphie et paléontologie des carrières du Brouillard et de Hucheloup (Ecouflant, Maine-et-Loire). *Annales de paléontologie* 99: 361–374. <https://doi.org/10.1016/j.anpal.2013.10.001>.
- Néraudeau D, Saint Martin S, Batten DJ, Colin J-P, Daviero-Gomez V, Girard V, *et al.* 2016. Palaeontology of the upper Turonian paralic deposits of the Sainte-Mondane Formation, Aquitaine Basin, France. *Geologica Acta* 14: 53–69.
- Néraudeau D, Perrichot V, Batten D, Boura A, Girard V, Jeannau L, *et al.* 2017. Upper Cretaceous amber from Vendée, north-western France: Age dating and geological, chemical, and palaeontological characteristics. *Cretaceous Research* 70: 77–95.
- Nohra YA, Perrichot V, Jeanneau L, Le Pollès L, Azar D. 2015. Chemical characterization and botanical origin of French Ambers. *Journal of Natural Products* 78(6): 1284–1293. <https://doi.org/10.1021/acs.jnatprod.5b00093>.
- Otto A, Simoneit BRT. 2002. Biomarkers of Holocene buried conifer logs from Bella Coola and north Vancouver, British Columbia, Canada. *Organic Geochemistry* 33(11): 1241–1251. [https://doi.org/10.1016/S0146-6380\(02\)00139-0](https://doi.org/10.1016/S0146-6380(02)00139-0).
- Peris D, Pérez-de la Fuente R, Peñalver E, Delclòs X, Barrón E, Labandeira CC. 2017. False Blister Beetles and the expansion of gymnosperm-insect pollination modes before Angiosperm dominance. *Current Biology* 27: 1–8.
- Perrichot V. 2005. Environnements paraliques à ambre et végétaux du Crétacé Nord-Aquitain (Charentes, Sud-Ouest de la France). *Mémoires Géosciences Rennes* 118: 1–310.
- Peyrot D, Barrón E, Polette F, Batten DJ, Néraudeau D. 2019. Early Cenomanian palynofloras and inferred resiniferous forests and vegetation types in Charentes (southwestern France). *Cretaceous Research* 94: 168–189.
- Philippe M. 1995. Bois fossiles du Jurassique de Franche-Comté (nord-est de la France) : systématique et biogéographie. *Palaeontographica Abteilung B* 236(1/3): 45–103.
- Philippe M, Bamford M. 2008. A key to morphogenera used for Mesozoic conifer-like woods. *Review of Palaeobotany and Palynology* 148: 184–207.
- Pocock SAJ. 1972. Palynology of the Jurassic sediments of Western Canada. Part 2. Marine species. *Palaeontographica Abteilung B* 137: 85–153.
- Poinar GO Jr. 1992. Life in amber. Stanford University Press, 368 p.
- Poinar GO Jr. 2010. *Cascoplecia insolitis* (Diptera: Cascopleciidae), a new family, genus, and species of flower-visiting, unicorn fly (Bibionomorpha) in Early Cretaceous Burmese amber. *Cretaceous Research* 31: 71–76.
- Polette F. 2019. Les assemblages palynologiques continentaux du Crétacé inférieur de France (Tithonien-Cénomanién): paléoenvironnements, paléoclimats, stratigraphie, et taxinomie. Thèse, université de Rennes, 2 tomes, 592 p. (inédit).
- Polette F, Licht A, Cincotta A, Batten DJ, Depuydt P, Néraudeau D, *et al.* 2019. Palynological assemblage from the lower Cenomanian plant-bearing Lagerstätte of Jaunay-Clan Ormeau-Saint-Denis (Vienne, western France): stratigraphic and paleoenvironmental implications. *Review of Palaeobotany and Palynology* 271: 1–21.
- Pons D, Boureau E, Broutin J. 1976. Nouvelles études paléobotaniques des environs d'Angers I. *Eretmophyllum andegavense* nov. sp., ginkgoale fossile du Cénomanién. In: *Comptes rendus du 9<sup>e</sup> Congrès national des Sociétés savantes*. Section Sciences, Nantes, pp. 367–369.
- Pons D. 1979. Les organes reproducteurs de *Frenelopsis alata* (K. Feistm) Knobloch, Cheirolepidiaceae du Cénomanién de l'Anjou, France. In: *Comptes rendus du 10<sup>e</sup> Congrès national des Sociétés savantes*. Section Sciences, Bordeaux, pp. 209–231.
- Proctor MCF, Tuba Z. 2002. Poikilohydry and homiohydric: antithesis or spectrum of possibilities? *New Phytologist* 156: 327–349.
- Rasband WS. 1997–2013. ImageJ. Bethesda, Maryland, USA: U.S. National Institutes of Health. <http://rsb.info.nih.gov/ij/>.
- Ravn RL. 1995. Miospores from the muddy sandstone (upper Albian), wind river basin, Wyoming, USA. *Palaeontographica Abteilung B* 234: 41–91.
- Ravn RL, Witzke BJ. 1995. The palynostratigraphy of the Dakota Formation (?Late Albian-Cenomanian) in its type area, northwestern Iowa and northeastern Nebraska, USA. *Palaeontographica Abteilung B* 234: 93–171.
- Redois F, Durand M, Fleury R, Mellier B, Moreau J-D, Néraudeau D, *et al.* 2016. Les argiles ligniteuses du Cénomanién de Hucheloup (Ecouflant, Maine-et-Loire). In: *Colloque du Groupe français du Crétacé, Musée Vert*, avril 2016, Le Mans, pp. 75–76.
- Rusea G, Claysius K, Runi S, Joanes U, Haja Maideen KM, Latiff A. 2009. Ecology and distribution of Lycopodiaceae Mirbel in Malaysia. *Blumea* 54: 269–271.
- Saint Martin J-P, Saint Martin S. 2018. Exquisite preservation of a widespread filamentous microorganism from French Cretaceous ambers: a key for review of controversial fossil. *Comptes Rendus Palevol* 17: 415–434.
- Saint Martin S, Saint Martin J-P, Girard V, Grosheny D, Néraudeau D. 2012. Filamentous micro-organisms in Upper Cretaceous amber (Martignes, France). *Cretaceous Research* 35: 217–229.
- Saint Martin S, Saint Martin J-P, Girard V, Néraudeau D. 2013a. Organismes filamenteux de l'ambre du Santonien de Belcodène (Bouches-du-Rhône, France). *Annales de paléontologie* 99: 339–360.
- Saint Martin J-P, Saint Martin S, Néraudeau D. 2013b. L'ambre associé aux lignites cénomaniens du Sarladais (Dordogne, SO France). *Annales de paléontologie* 99: 289–300.
- Samuel E, Gaillard MG. 1984. Les gisements à flore fossile d'âge Crétacé supérieur en France : localisation, stratigraphie et essai de

- corrélations des données macro- et microfloristiques. *Bulletin mensuel de la Société linnéenne de Lyon* 53<sup>e</sup> année 6: 213–223.
- Schmidt AR, Schäfer U. 2005. *Leptotrichites resinatus* new genus and species: a fossil sheathed bacterium in Alpine Cretaceous amber. *Journal of Paleontology* 79: 175–184.
- Schrank E. 2010. Pollen and spores from the Tendagru Beds, Upper Jurassic and Lower Cretaceous of southeast Tanzania: palynostratigraphical and paleoecological implications. *Palynology* 34: 3–42.
- Singh C. 1971. Lower Cretaceous microfloras of the Peace River area, Northwestern Alberta. *Bulletin of the Research Council of Alberta Bulletin* 28: 1–522.
- Singh C. 1983. Cenomanian microfloras of the Peace River area Northwestern Alberta. *Bulletin of the Research Council of Alberta Bulletin* 44: 1–322.
- Smith AR, Pryer KM, Schuettpelz E, Korall P, Schnieffer H, Wolf PG. 2006. A classification of extant ferns. *Taxon* 55: 705–731.
- Stearr DC, Strullu-Derrien C, Philippe M, Krieger J, Stevens L, Spencer ART, *et al.* 2020 (submitted). New evidence of the architecture and affinity of fossil trees from the Jurassic Period Purbeck Forests of southern England.
- Thévenard F, Gomez B, Daviero-Gomez V. 2005. Xeromorphic adaptations of some Mesozoic gymnosperms. A review with paleoclimatological implications. *Comptes Rendus Palevol* 4: 67–77.
- Vakhrameev VA, Doludenko MP. 1977. The Middle–Late Jurassic boundary, an important threshold in the development of climate and vegetation of the Northern Hemisphere. *International Geology Review* 19: 621–632.
- Van Konijnenburg-Van Cittert JHA. 1971. *In situ* gymnosperm pollen from the Middle Jurassic of Yorkshire. *Acta Botanica Neerlandica* 20: 1–97.
- Van Konijnenburg-Van Cittert JHA. 2002. Ecology of some Late Triassic to Early Cretaceous ferns in Eurasia. *Review of Palaeobotany and Palynology* 119: 113–124.
- Waksmundzka M. 1981. Palynological analysis of Lower Cretaceous sediments from Kujawy (Poland). *Acta Paleontologica Polonica* 26: 257–280.
- Walker JW, Walker A. 1984. Ultrastructure of Lower Cretaceous angiosperm pollen and the origin and early evolution of flowering plants. *Annals of the Missouri Botanical Garden* 71: 464–521.
- Wetzel W. 1953. Mikropaläontologische Untersuchung des schleswig-holsteinischen Bernsteins. *Neues Jahrbuch für Geologie und Paläontologie* H7: 11–321.

**Cite this article as:** Néraudeau D, Saint Martin J-P, Saint Martin S, Jeanneau L, Moreau J-D, Philippe M, Polette F, Gendry D, Brunet J, Tréguier J. 2020. Amber- and plant-bearing deposits from the Cenomanian of Neu (Mayenne, France), *BSGF - Earth Sciences Bulletin* 191: 39.